**ISAS - INTERNATIONAL SCHOOL FOR ADVANCED STUDIES**

# Intergalactic Medium at High Redshifts

Thesis presented by

Jianmin Liu

for the degree of Master

Supervisor: Professor Dennis Sciama

S.I.S.S.A. - I.S.A.S.

*Astrophysics Sector*

Academic year 1994-95

**SISSA - SCUOLA INTERNAZIONALE SUPERIORE DI STUDI AVANZATI**
TRIESTE
Strada Costiera 11

**TRIESTE**

# Intergalactic Medium at High Redshifts

Thesis presented by

**Jianmin Liu**

for the degree of Master

**Supervisor: Professor Dennis Sciama**

**S.I.S.S.A. - I.S.A.S.**

*Astrophysics Sector*

Academic year 1994-95

# Acknowledgements

I am very grateful to Professor Dennis Sciama, my supervisor, for his guidance and for his patience with my english. I also thank Dr. Ewa Szuszkiewicz for her assistance and continuous encouragement of my research work. I am greatly indebted to Dr. Avery Meiksin for his invaluable advice and insightful discussions. I appreciate Dr. Alejandra Melfo for her carefully reading the first part of this thesis which improved its readability.

# Contents


**1 Introduction** ..... 1

**2 The Guun-Peterson Effect of the Diffuse IGM** ..... 8

2.1 Basic Theory ..... 9
2.2 HI G-P Effect ..... 10
2.3 HeI G-P Effect ..... 11
2.4 HeII G-P Effect ..... 12
2.4.1 Line Blanketing ..... 13
2.4.2 G-P Trough ..... 14
2.4.3 Proximity Profile of Intergalactic HeII Resonance Absorption ..... 15

**3 Ionizing Background Radiation Field and Reionization of Intergalactic Medium (IGM)** ..... 17

3.1 Source of the Ionizing Background Radiation Field ..... 19
3.1.1 QSOs ..... 19
3.1.2 AGNs ..... 19
3.1.3 Young Star in Galaxies ..... 20
3.1.4 Decay Neutrinos ..... 20
3.1.5 IGM Emission ..... 20
3.2 Calculation of the Ionizing Background Radiation Field ..... 21
3.2.1 Absorption by the Diffuse IGM ..... 22
3.2.2 Absorption by the Clumped IGM ..... 23
3.3 Evolution of the IGM ..... 26
3.3.1 Reionizing Epoch ..... 26
3.3.2 Evolution of the IGM after Overlaping ..... 29

**4 Lyα Clouds (LCs)** ..... 33

4.1 HI Equivalent Width Distribution ..... 33
4.2 HI Column Density Distribution ..... 34
4.3 Evolution of Number Density with Redshift ..... 35

4.4 Temperature of the LCs ..... 37
4.5 Size of the LCs ..... 39
4.6 Spatial Distribution of the LCs ..... 40
4.7 Metallicity of the LCs ..... 43
4.8 Proximity Effect ..... 45
4.9 Fundamental Equations for Structure and Evolution of the LCs ..... 47
4.10 Confinement Mechanisms ..... 49
4.10.1 Gravity Confinement ..... 50
4.10.2 Pressure Confinement ..... 50
4.10.3 Mixed Gravity and Pressure Confinement ..... 51

**5 Metal Absorption Systems (MASs)** ..... **53**

5.1 Photoionization Model ..... 56
5.2 Evolution of Number Density of with Redshift ..... 57
5.3 HI Column Density Distribution of the LLSs ..... 60
5.4 Equivalent Width Distribution of MgII or CIV Absorption Lines ..... 61
5.5 Spatial Distribution and Correlation with the QSOs ..... 62
5.6 Metallicity of the MASs ..... 64
5.7 Properties of the MASs ..... 66
5.8 Relationship between the MASs and Galaxies ..... 68
5.9 Comparison with the LCs ..... 70

# Chapter 1

# Introduction

It is universally agreed that the early Universe was very homogeneous at an early epoch. The mass density perturbation at decoupling was of the order of $\sim 10^{-3}$. One of the strong evidences is that the anisotropies of the temperature of cosmic microwave background radiation $\Delta T/T$ on both large and small scales are less than $10^{-3}$ (Smoot et al. 1992; Dragovan et al. 1994; Readhead et al. 1989). On the other hand, the present Universe is very lumpy on small scales. For example, the density within a galaxy is about $10^5$ the average density of the Universe, and that within a cluster of galaxies is about $10^2$ to $10^3$ times the average density in the Universe. It is natural to ask what mechanisms response for the observable clumped structures today. It is widely believed that gravitational instability from primordial small perturbations causes that structures in our Universe today.

According to the standard picture of gravitational instability, there exists a critical mass, so called Jeans mass $M_J$, such that perturbations of mass less than $M_J$ are stable against gravitational collapse and still remain in diffuse status, whereas those of mass greater than $M_J$ are unstable and collapse. The collapse time scale depends on the mass, the greater the mass is, the faster it collapses. Therefore, some of them with greater mass have become gravitationally bound objects, some still expand with the Hubble flow. So, roughly speaking, the Universe is a sea with bound objects surrounded by in a sense diffuse medium. The clumped structures, based on their properties, are classified as clusters of galaxies, galaxies and so on.

The absorber systems inferred from the absorption lines in the spectrum of QSO could be these objects whose mass, density, length scale and other

properties are similar to absorbers', such as dwarf irregular galaxies, primordial intergalactic clouds, intergalactic shocks or primordial halos of normal galaxies. The relatively uniformly distributed medium is usually called a diffuse component of intergalactic medium (IGM). Although there is no definite observational evidence that the diffuse IGM component exists in substantial quantities, there is much theoretical speculation supporting or requiring it. For instance, in both the hot dark matter (HDM) model and the cold dark matter (CDM) model of the Universe (e.g., Chiang, Ryu, & Vishniac 1989; Ryu, Vishniac, & Chiang 1990; Cen et al. 1990), galaxies were formed efficiently only at redshift $z < 2$, so a large fraction of the primordial hydrogen and helium should not have been collapsed into galaxies before or at that redshift.

A calculation by Shapiro et al. (1991) showed that at redshift $z \sim 2$, about half of the total baryonic matter was not collapsed into galaxies and thus was left in intergalactic space as a diffuse IGM component. More recently, Shapiro et al. (1994) performed a detailed calculation to investigate the coupled evolution of the IGM and the emerging structure in the context of the CDM model. They showed that a significant fraction of baryons remain uncollapsed in the IGM after redshift $z \sim 5$ even if there is no reheating epoch. If energy releases by the collapsed baryon fraction are included, then this reionization will inhibit baryon collapse so that more than half of the baryon fraction remain in the IGM at $z \sim 4$.

As a consequence of the IGM existing in substantial quantities, its bremsstrahlung X-radiation, free-free absorption, scintillation on radio sources, or the Zel'dovich-Sunyaev effect could be observed. Up to now, no positive detection has been reported along these directions (for reviews, see Field 1972; Blades, Turnshek, &Norman 1988). The more sensitive method to detect the IGM is through its selective absorption on the light of a background object. The recent detection (Bi 1991) by looking for 21 cm absorption in spectrum of radio source set an upper limit to the density $\Omega(HI) \leq 4.5 \times 10^{-3} h^{-1}$.

Another more prominent absorption in the search for IGM is the resonant Ly$\alpha$ absorption. The feature of absorption by the IGM left in the spectrum of QSO depends on the feature of distribution of the IGM, clumped or diffuse. As a photon travels through the diffuse IGM component from a high redshift QSO to us and redshifts, when its energy coincides with the resonant energy of Ly$\alpha$, it is probably absorbed. The combination of all absorption occurred at different redshifts produces an absorption trough in the measured

spectrum of the QSO. As it was firstly pointed out by Guun &Peterson in 1965, it is called Guun-Peterson (G-P) effect. It is usual to use the Guun-Peterson optical depth $\tau_{GP} = -ln(I_c/I_{extr})$ to represent the amplitude of the G-P effect. From an observational point of view $\tau_{GP}$ is measured by the ratio between the local continuum level shortward of the Lyα emission and the extrapolated continuum level longward of the Lyα emission, where the continuum is unaffected by the IGM absorption. It is apparent that a richer diffuse IGM component causes a stronger G-P absorption trough, i.e. a greater $\tau_{GP}$. Therefore, searching for $\tau_{GP}$ could provide a clue to derive the amount of diffuse IGM. Because the richest elements of the IGM are hydrogen and helium, detecting G-P effect is concentrated on hydrogen and helium. So far, a lot of G-P tests have been performed. Steidel & Sargent (1987) have shown that G-P optical depth of hydrogen $\tau_{GP}(HI) \simeq 0.02 \pm 0.03$ at $z = 2.6$: Giallongo & Cristiani (1990) and Cristiani et al. (1993) claimed that no evidence for a HI G-P effect (i.e. $\tau_{GP}(HI) < 0.1$) up to $z = 5$. A more stringent and direct upper limit to G-P effect given by Giallongo et al. 1992, 1994 is at $z = 4.3$ $\tau_{GP}(HI) \simeq 0.02 \pm 0.03$. It is natural to extend this attempt to searching for the helium absorption troughs at far-untraviolet wavelengths. Searchs for a HeI Lyα (584 Å) absorption trough have been negative (Tripp. Green, & Bechtold 1990; Reimers & Vogel 1993), but Jakobsen et al. (1994) have recently reported an evidence for a HeII G-P trough in the spectrum of the QSO 0302-003 ($z_{em} = 3.286$). They argue that the absorption edge they observed, with $\tau > 1.7$ at 90% confidence, is probably due to HeII in the diffuse IGM, rather than HeII line-blanketing (Madau & Meiksin 1994 ) arising from Lyα forest clouds or a foreground hydrogen Lyman limit system at much lower redshift. More recently, Tytler (1995) reported that the *Hubble Space Telescope* (HST) Faint Object Spectrograph (FOS) detected absorption with optical depth $\tau(HeII) \simeq 1.0 \pm 0.2$ in the spectrum of the z=3.185 QSO 1935-67.

The detected small $\tau_{GP}(HI)$ indicates that $\Omega(HI) \leq 10^{-8}$, where $\Omega(HI)$ is the neutral hydrogen density in the diffuse IGM in units of the critical density. This is far below the baryon density inferred from standard Big Bang nucleosynthesis, $\Omega_b = 0.0125h^{-2}$ (Walker et al. 1991) (here $h$ is the Hubble constant in units of 100 $Kms^{-1}Mpc^{-1}$). This paucity of HI in the diffuse IGM can be interpreted either as an indication that the diffuse IGM was neutral but contained an undetectably small fraction of the total baryon density of the Universe, or else that it was highly ionized.

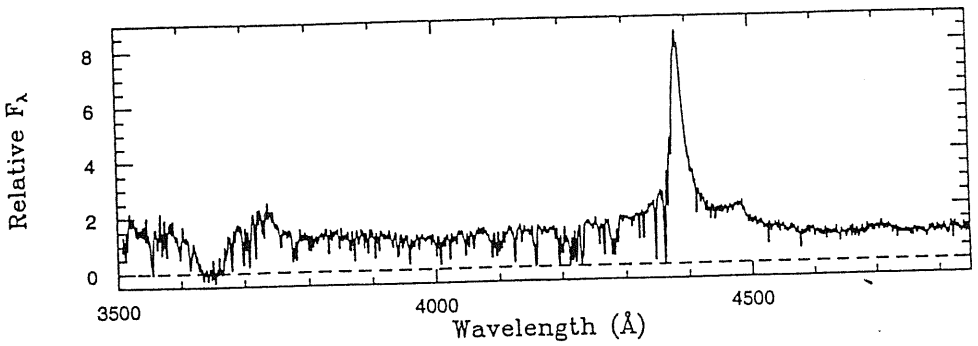


Figure 1.1: Spectrum of a quasar at redshfit $z_{em} = 2.6$ (Wolfe et al. 1993). The broad peak is the atomic hydrogen Lyman-$\alpha$ emission line from the quasar. Most of the absorption features at shorter wavelengths are produced by resonant Lyman-$\alpha$ scattering in gas clouds along the line of sight between us and the quasar.

The usual interpretation of the G-P constraint is that the IGM was highly ionized. Presuming that the IGM was largely neutral following the epoch of recombination at $z \sim 10^3$, a highly ionized IGM at $z \leq 5$ implies that the Universe must have passed through an *epoch of reionization*, most likely caused by energy released during the gravitational collapse of the matter in the Universe. There are a lot of possible objects which may provide ionizing photons, such as QSOs , decay neutrinos, primeval galaxies, or Population III stars (Shapiro & Giroux 1987; Miralda & Ostriker 1990; Madau & Meiksin 1991; Sciama 1990, 1993, 1994a, b;). Alternatively, the G-P test may be satisfied if the IGM has been shock-heated by explosions (Ostriker & Ikeuchi 1983). The different kind of source has different emissivity and spectral feature, and the spectral shape plays an important role in determining the fraction of the ionization stages of hydrogen, helium and metal elements. Therefore, comparison of $\tau_{GP}(HI)$ with $\tau_{GP}(HeII)$ provides a way to derive the spectral shape of the background ionization radiation.

On the other hand, as a photon travels through the clumped IGM, the absorption invoked by an electronic transition from the $1s$ to the $2p$ states produces a discrete absorption line, instead of an absorption trough, in the spectrum of the QSOs (Sargent et al. 1980) (SYBT). Indeed, one of the most striking features of the spectra of high-redshift QSOs is that there are a lot

of narrow absorption lines with wavelengths shorter than Ly$\alpha$ emission (in the rest frame) (Figure 1.1). In this region(commonly known as the Ly$\alpha$ forest) the majority of absorption lines are Ly$\alpha$ and the HI coulds giving rise to them are referred to colloquially as the Ly$\alpha$ clouds (LCs). A small proportion of the lines can be identified with metal elements.

In order to have an apparent understanding of absorbers, we briefly summarize some their properties as follows:

1. The absorption arises as the QSO light passes through tenuous gas clouds, which are transparent, except at the few specific wavelengths at which absorption lines occur. All lines arising in one gas clouds are known collectively as a system.

2. While the absorption by a spectral line occurs at its laboratory wavelength $\lambda_{lab}$, the expansion of the Universe results in a redshfit in all wavelengths. The redshfit is defined as

$$(1 + z_{abs}) = \lambda_{obs}/\lambda_{lab}, \tag{1.1}$$

where $(1 + z_{abs})$ is the linear factor by which the Universe has expanded since the time of the absorption.

3. QSOs have now been observed out to redshfits of $z_{em} \approx 5$, and absorption has been seen at all redshfit up to this value. The probability that an individual photon is absorbed as it passes through a cloud is near zero for most photons, but can rise to close to one at resonant wavelengths. This probability depends on the number of ions per square centimeter along the line of sight, usually called column density.

4. The width of a line is caused by Doppler effect of the velocities of the individual ions causing the absorption, due to gas temperature and bulk motions. Most lines are narrow with widths $\leq 1\mathring{A}$, corresponding to a velocity dispersion in the range 1 to 100 $kms^{-1}$. However, the total amount of absorption, known as equivalent width, is not affected by this redistribution in wavelength.

5. Some 99% of systems show only lines of HI, neutral hydrogen (Sargent et al. 1980). QSOs at $z_{em} \geq 3$ show over a hundred HI Lyman-$\alpha$ absorption lines.

Observations have revealed that the neutral hydrogen column densities span a range of at least nine orders of magnitude, from $10^{12.5}$ to $10^{22}$ $cm^{-2}$, where the minimum value corresponds to detection threshold in the best

available data. Traditionally, the numerous absorption lines systems are divided, according to their neutral hydrogen column densities, into four categories:

1. **Ly$\alpha$ Clouds (LCs)**

   The LCs roughly have the HI column density $N(HI) < 1.6 \times 10^{17}\, cm^{-2}$, corresponding to Lyman continuum optical depths $\tau < 1$ at $\lambda < 912\mathring{A}$. One of their distinct characters is relatively poor in metal elements.

2. **Lyman Limit Systems (LLSs)**

   Generally speaking, the LLSs have the HI column density $N(HI) > 1.6 \times 10^{17}\, cm^{-2}$, corresponding to Lyman continuum optical depths $\tau > 1$ at $\lambda < 912\mathring{A}$, frequently, metal absorption lines may be seen in the spectra of QSOs. Unlike the LCs, the LLSs produce strong continuous absorption at all wavelength $\lambda_{obs} \leq (1 + z_{abs})912\mathring{A}$. Although they are scarcer than the LCs, they are important because they are easier to detect than any other systems. They are also the major source of ultraviolet opacity in the Universe.

3. **Damped Ly$\alpha$ systems (DSs)**

   The DSs have the HI column density $N(HI) > 10^{20}$ and are metal rich systems. Their column densities are similar to the column density in the gaseous disks of present spiral galaxies. The damping wings of Ly$\alpha$ lines are prominent for the DSs. They are believed to arise in high-redshfit disc galaxies (Wolf et al. 1986). The LLSs and the DSs are subsets of the metal absorption systems (MASs).

4. **Broad Absorption Line Systems (BALs)**

   The BALs are found to have unexceptionally wide absorption lines. It is almost universally agreed that they are caused by expanding gas which has been ejected from the QSO since they are found at velocities only few thousand $kms^{-1}$ less than QSOs, never at $z_{abs} \ll z_{em}$. The BAL is totally different from other populations of absorbers (e.g. the LC and the LLS). In this thesis, we will ignore the BAL.

The different regimes of HI density appear to have different properties. At the low end $[N(HI) < 10^{15}\, cm^{-2}]$, search for metal element absorption in

composite spectra (e.g. Lu 1991; Cowie et al. 1995) suggest that the metal abundances are much low compared to solar. These clouds seem to be only weakly clustered, on velocity scales below $200\,kms^{-1}$ (e.g. Webb 1987; Chernomordik 1995; Cristiani et al. 1995a Elowitz et al. 1995). Systems with HI column densities above $\sim 10^{17}\,cm^{-2}$ exhibit a conspicuous discontinuity at the Lyman limit. These systems frequently exhibit absorption lines due to several ionization stages of the metal elements, and complex velocity structure (e.g. Blades 1988). The apparently different clustering characteristics have led to the speculation that the Lyman clouds and metal absorption systems are associated with physically distinct population of objects (Sargent et al. 1980). It is, however, not clear whether the differences in clustering reflect intrinsic differences or observational limitations.

An alternative viewpoint (e.g. Bergeron & Borssè 1984; Tytler 1987) is that the LCs, LLSs and DSs are of the same population and have the same origin. The evidence for a single population is that the observed HI column density distribution may described by a featureless power law over whole column density range from $10^{12.5}$ to $10^{22}\,cm^{-2}$. This seems an unlike coincidence if one accepts that completely different objects contribute to the observed distribution. Tytler (1987) in particular emphasized this point. This year, the measured considerable metallicity of the LCs (Cowie et al. 1995; Savaglio & Webb 1995) and the observed clustering property of the LCs (Chernomordik 1995; Cristiani et al. 1995a; Elowitz et al. 1995) seem to be in favor of Tytler's point of view.

Though there exist uncertainties on the origin and structure of QSO absorption systems, they potentially convey valuable information about the Universe at large redshifts. Specific questions addressed by QSO absorption systems include: How many subpopulations are represented among the observed intervening system? What types of environments are sampled by the intervening absorbers (intergalactic medium, voids, walls, clusters of galaxies, isolated galaxies)? What is the large-scale spatial distribution of the absorbers)? What is the distribution of the physical conditions (e.g. column density, velocity dispersion, small-scale clustering, ionization, chemical composition, and so on) and do these properties vary with redshfit?

# Chapter 2

# The Guun-Peterson Effect of the Diffuse IGM

An important source of information on the distribution and the physical state of the IGM up to redshift $z \simeq 5$ is provided by the study of the absorption spectra of high-redshift QSOs. The G-P effect is the most sensitive method known for the detecting smoothly distributed neutral IGM. The Ly$\alpha$ resonance scattering cross section is so large that a very small amount of the diffuse IGM in the line of sight of distant QSO will dramatically depress the continuum blueward of the Ly$\alpha$ emission line and should be easily observable (Guun-Peterson 1965). Any null detection of such continuum drop aside from the numerous discrete absorption line-blanketing by the LCs will set a striking limit for the atomic number density of the diffuse neutral IGM. The absence of the long-looked-for absorption trough shortward of the QSO Ly$\alpha$ hydrogen emission, caused by Ly$\alpha$ absorption of diffuse intergalactic neutral hydrogen, implies that the IGM is highly ionized. The estimate of the true continuum level shortward of the Ly$\alpha$ emission is made difficult by a crowd of narrow absorption lines due to the intervening LCs (Steidel & Sargent 1987). The previous measures on the G-P effect rely on the knowledge of the statistical properties of the LC redshift and column density distributions (Jenkins & Ostriker 1991). More recently, some new more stringent techniques have been developed for measuring G-P effect (Giallongo et al. 1994; Fang & Crotts 1995).

## 2.1 Basic Theory

The easier way to compute the effect of scattering by a smoothly distributed neutral IGM is to write the scattering cross section as a function of frequency through the Ly$\alpha$ resonance as

$$\sigma(\nu) = \frac{\pi e^2}{mc} f g(\nu - \nu_\alpha), \tag{2.1}$$

where $f$ is the oscillator strength, and $g$ is the profile function, which is strongly peaked at $\nu = \nu_\alpha$, and has unit integral

$$\int_{-\infty}^{\infty} g(x)dx = 1. \tag{2.2}$$

Without loss of generality, we simplify

$$\sigma(\nu) = \frac{\pi e^2}{mc} f \Delta(\nu - \nu_\alpha), \tag{2.3}$$

where $\Delta$ is a Dirac delta function.

Now let us get the optical depth for absorption of light that passes through the local Ly$\alpha$ resonance, as the radiation moves toward us through a smoothly distributed IGM. The G-P optical depth at observed frequency $\nu_0$ is

$$\tau_{GP} = \int \sigma(\nu_0(1+z))n(z)dl = \int_0^z \sigma(\nu_0(1+z))n(z)\frac{dl}{dz}dz. \tag{2.4}$$

Putting

$$\frac{dl}{dz} = \frac{cH_0^{-1}}{(1+z)^2(1+2q_0z)^{1/2}} \tag{2.5}$$

and Eq.(2.3) into Eq.(2.4), we obtain

$$\tau_{GP} = \frac{\pi e^2 \lambda_\alpha f}{mcH_0} \frac{n(z)}{(1+z)(1+2q_0z)^{1/2}}, \tag{2.6}$$

where $n(z)$ is the proper number density of the species which is measured (e.g. HI, HeI or HeII). Inversely, we have the following expression for $n(z)$ in terms of $\tau_{GP}$

$$n(z) = \frac{mcH_0}{\pi e^2 \lambda_\alpha f}(1+z)(1+2q_0z)^{1/2}\tau_{GP}. \tag{2.7}$$

It is apparent that we can get a constraint on the number density in diffuse IGM in terms of the G-P optical depth $\tau_{GP}$.

Table 2.1. Results of G-P Test

| | | z | $\tau_{GP}$ |
|---|---|---|---|
| Steidel & Sargent | 1987 | 2.6 | $\simeq 0.02 \pm 0.03$ |
| Webb et al. | 1992 | 4.1 | $\leq 0.04$ |
| Giallongo et al. | 1993 | $\leq 5$ | $\leq 0.1$ |
| Giallongo et al. | 1994 | 4.3 | $\simeq 0.02 \pm 0.03$ |
| Fang & Crotts | 1995 | 3.4 | $0.115 \pm 0.025$ |
| Cristiani et al. | 1995b | 3.8 | $\sim 0$ |

## 2.2 HI G-P Effect

A number of experiments have been carried out on HI G-P effects. The main results are summarized in Table 2.1. QSO spectra show not very pronounced decrease from what can be expected from an extrapolation of the long wavelength side of the QSO Lyα emission line, where the spectrum is not affected by resonant scattering. With high confidence, we can safely set an upper limit on the G-P optical depth, saying $\tau_{GP} \leq 0.1$ at high redshifts. The corresponding neutral hydrogen number density will be based on Eq.(2.7)

$$n(HI) = 2.4 \times 10^{-12} h(1+z)(1+2q_0 z)^{1/2}. \tag{2.8}$$

The ratio of this expression to the Einstein-de Sitter mass density $n = 1.12 \times 10^{-5} \Omega_B h^2 (1+z)^3 \, cm^{-3}$ scaled to the epoch z is

$$\Omega(HI) \leq 2 \times 10^{-7} h^{-1} (1+z)^{-2} (1+2q_0 z)^{1/2}. \tag{2.9}$$

This strikingly low limit on the density of neutral smoothly distributed hydrogen applies at redshifts near zero to $z \sim 5$. At the largest observed redshifts, crowding of the Lyα lines weakens the limit on $\tau$, but still we can conclude that at $z \sim 5$ the intercloud neutral hydrogen density is at least five orders of magnitude below the estimate for the baryon density from light element production (Walker et al. 1991).

## 2.3 HeI G-P Effect

Because helium is the second richest element in the Universe, it is natural to extend hydrogen G-P test to helium G-P test. Following the method outlined in the preceding sections, we can show that the total optical depth at a given redshift in HeI $\lambda 584\mathring{A}$ is given by

$$\tau_{GP}(He I) = 1.32 \times 10^{10} \frac{n_{He I}(z)}{h(1+z)(1+2q_0 z)^{1/2}}. \qquad (2.10)$$

Thus, if the continuum shortward of $\lambda 584(1+z)$ is depressed by $e^{\tau_{GP}}$, then the neutral helium number density at a given redshift can be obtained from Eq.(2.10). No G-P trough has been measured so far. Tripp et al.(1991) estimated that $\tau_{GP} < 0.21$ at the $3\sigma$. This limit requires that, for example, at emission redshift $z_{em} = 1.722$,

$$n(He I) \leq 7.1 \times 10^{-11} h\, cm^{-3} \qquad (q_0 = 0.5). \qquad (2.11)$$

No detected HeI G-P trough (Tripp et al. 1990; Beaver et al. 1991: Reimer et al. 1992) is not surprising. Assumed a suitable ionizing source (Bajtlik et al. 1988; Bechtold et al. 1994), which makes the diffuse IGM satisfy the HI G-P constraint, the photoionization models or the shock-heated models (Giroux & Shapiro 1994; Sciama 1994a, b; Miralda & Ostriker 1990; Shapiro 1989; Shapiro et al. 1987; Ikeuchi & Ostriker 1986; Ostriker & Ikeuchi 1983; Sargent et al. 1980) predict that the most of helium is in doubled ionized state and HeI is much fewer than HeII. For a photoionization model (based on ionization equilibrium).

$$\frac{n(He I)}{n(HI)} \approx 0.044 \frac{J_{HI}}{J_{He I}} \xi_{He II}, \qquad (2.12)$$

where the quantity $J_{HI}$ is a frequency-averaged intensity, weighted with the ionization efficiency factor $\sigma_{HI}/\nu$, and $J_{He I}$ is the analogous quantity for helium, and $\xi_{He II}$ is the fraction of HeII. If the intensity of ionization background is about the order of $10^{-21}\, ergs\, cm^{-2} s^{-1} Hz^{-1} sr^{-1}$, which is inferred from the proximity effect (Bajtlik et al. 1988;) (BDO), most of theories for the ionization of the diffuse IGM predict that $\xi_{He II} \leq 10^{-2}$. Therefore, the fraction of HeI is too small to get the useful information from HeI G-P test.

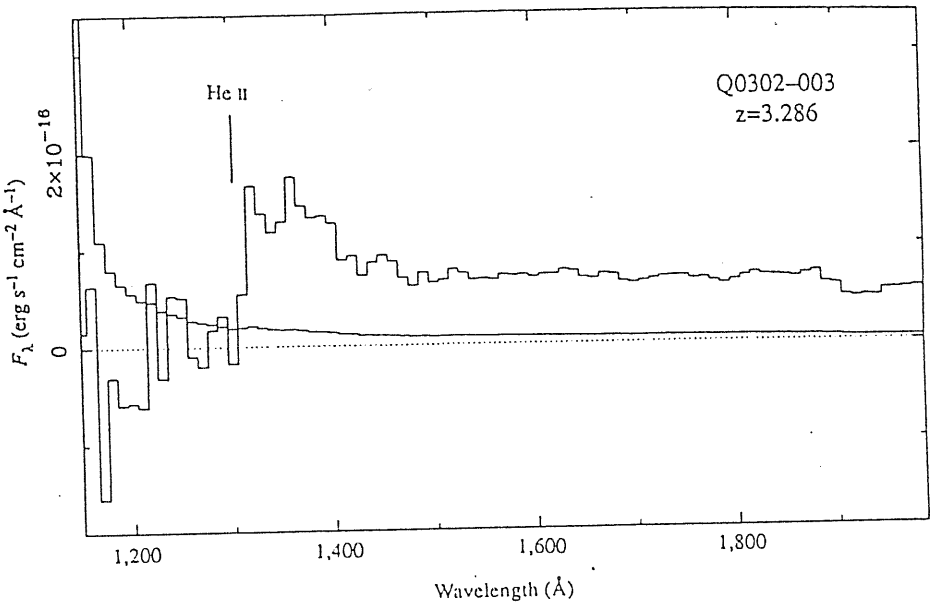


Figure 2.1: Flux ($F_\lambda$) and wavelength calibrated FOC far-UV prism spectrum (solid) of Q0302-003. The thin solid line gives the 1 $\sigma$ uncertainty per $\Delta$ = 10Å wavelength bin due to photon statistics. The absolute flux calibration should be accurate to within a factor of $\sim$ 2. The position of the HeII line in the quasar rest frame is marked. Taken from Jakobsen et al. (1994).

## 2.4 HeII G-P Effect

Instead of searching for the HeI G-P trough, people favor searching for HeII G-P trough. Indeed, Jakobsen et al. (1994) reported an evidence for a HeII G-P trough in the spectrum of the QSO 0302-003 (z=3.286) (Figure 2.1). However, at a modest spectral resolution (FOC), it is impossible to distinguish directly between smooth HeII 304Å absorption from the diffuse IGM and unresolved HeII 304Å line blanketing from the discrete LCs (Jakobsen et al. 1994; Madau & Meiksin 1994).

### 2.4.1 Line Blanketing

At wavelengths shortward of the rest-frame resonant line HeII 304Å, the source's continuum intensity is attenuated by the combined blanketing effect of numerous HeII absorption lines arising from the intervening discrete LC's. The average transmission over all lines of sight at the observed wavelength $\lambda_{obs} = \lambda_\alpha(1+z)$ may be expressed as $< e^{-\tau} >= e^{-\tau_{eff}}$, with the effective optical depth due to Poisson-distributed absorbers given by

$$\tau_{eff}(z) = \frac{1+z}{\lambda_\alpha}\int_{W_{min}}^{W_{max}} (\frac{\partial^2 N}{\partial W \partial z})_{HeII} W dW \tag{2.13}$$

(Paresce, McKee, & Bowyer 1980), where $(\partial^2 N/\partial W \partial z)_{HeII}$ is the HeII rest equivalent width distribution function. If known $(\partial^2 N/\partial W \partial z)_{HeII}$, it is easy to obtain HeII line blanketing effect by directly integrating Eq.(2.13). At prsent, we have no direct knowledge of the equivalent width distribution function for HeII. Fortunately, the equivalent width distribution function for HI is known as follows,

$$(\frac{\partial^2 N}{\partial W \partial z})_{HI} = \begin{cases} 40.7 exp(-W/W_*)(1+z)^{2.46} & (0.2 < W < 2\mathring{A}) \\ 11.4(-W/W_*)^{-1.5}(1+z)^{2.46} & (W_{min} < W < 0.2\mathring{A}), \end{cases} \tag{2.14}$$

where $W_* = 0.3\mathring{A}$ (Murdoch et al. 1986). So, in order to compute the HeII line blanketing effect, it is a critical point to transfer the HI rest equivalent width distribution function into HeII's. Obviously, this transformation relies on the spectral shape of the ionization background if it is assumed that photoionization is responsible for the ionization of the IGM. For an optical thin absorber, the ratio of column densities of $N_{HeII}$ and $N_{HI}$ is given simply by the assumption of photoionization equilibrium

$$\frac{N_{HeII}}{N_{HI}} \sim 0.54 S_L, \tag{2.15}$$

where $S_L = J_{HI}/J_{HeII}$, called the softness paramter (Madau & Meiksin 1994). Based on Eq.(2.15), a column density distribution function for HeII may be obtained from that for HI. Then, using a curve of growth analysis, $(\partial^2 N/\partial W \partial z)_{HeII}$ may be finally derived from HeII column density distribution function.

We want to mention here that the Doppler broadening of the absorption lines plays a considerable role in transferring the column density distribution

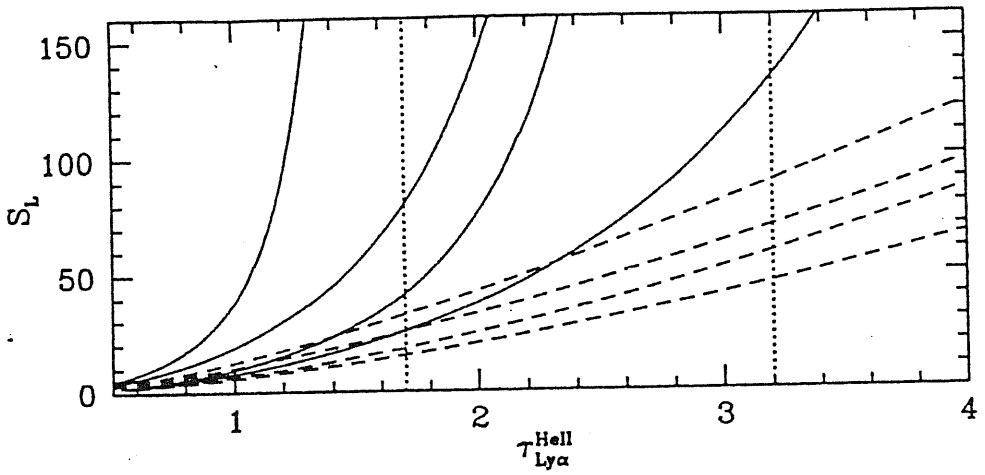


Figure 2.2: The softness parameter $S_L$ as a function of HeII optical depth for $b^{HI} = 35\,kms^{-1}$. The solid curves represent the effective opacity from line blanketing. The dash curves show the corresponding total optical depths including a contribution from the HeII G-P effect. To produce the observed opacity at HeII edge, the minimum value of $S_L$ is 18. Taken from Madau & Meiksin (1994)

function to equivalent width function. It is unknown whether the Doppler broadening is a result of bulk motion within the absorbers or thermal velocity. One can parameterize the HeII Doppler width as

$$b^{HeII} = \xi b^{HI}, \tag{2.16}$$

where $\xi = 0.5$ corresponding to thermal broadening, and $\xi = 1$ corresponding to bulk motion. Combining the Eqs.(2.13), (2.14), (2.15) and relying on the curve of growth analysis, we can, in principle, compute the HeII line blanketing effect (Figure 2.2).

### 2.4.2 G-P Trough

The optical depth of a HeII G-P absorption trough from the diffuse intergalactic helium is given by

$$\tau_{GP}(HeII) \sim 25(\frac{1+z}{4.3})^{4.5}\Omega_D^2 h_{50}^3 S_L J_{912,-21}^{-1} \tag{2.17}$$

(Meiksin & Madau 1993; Madau & Meiksin 1994), for an Einstein-de Sitter Universe with $H_0 = 50h_{50}\,kms^{-1}Mpc^{-1}$, and a contribution of the diffuse IGM to the critical density of $\Omega_D$. With $S_L \sim 50$ and $\Omega_D h_{50}^2 \sim 0.05$ (Walker et al. 1991), we have $\tau_{GP}(HeII) \sim 3$. Even for $J_{912,-21}$ as high as 3, the $1\sigma$ upper limit from proximity effect estimates (Bajitlik et al. 1988; Lu et al. 1991). the HeII G-P optical depth would be near unity.

### 2.4.3 Proximity Profile of Intergalactic HeII Resonant Absorption

An important point is to distinguish the contributions from discrete clumped LCs and a smoothly distributed IGM. Theoretically, the diffuse IGM produces a smooth absorption trough, whereas discrete absorbers form discrete absorption lines although these absorption lines are quite crowded at high redshifts. Unfortunately, however, at the current spectral resolution of FOC. we cannot distinguish directly between HeII 304Å absorption trough from the diffuse IGM and HeII 304Å line blanketing from the discrete LCs. More recently, Giroux, Farada & Shull (1995) suggested that the study of the proximity profile of HeII resonance absorption toward high redshift QSOs could provide a way to distinguish them. Close to the QSO, the number density of HeII is alter from that expected if it is photoionized solely by the metagalactic background radiation. Therefore,

$$\frac{n(HeII)}{n_B(HeII)} \sim \frac{J_B}{J_B + J_Q}, \tag{2.18}$$

where subscript $_B$ represents the value corresponding to background. The mean intensity of the ionizing continuum $J_Q$ at a given redshift $z$ from the observed value of $f_Q$ is

$$J_Q = \frac{f_Q}{4\pi}\frac{(1+z)^5}{(1+z_Q)}\left[\frac{(1+z_Q)^{0.5}-1}{(1+z_Q)^{0.5}-(1+z)^{0.5}}\right]^2 \tag{2.19}$$

(BDO 1988). Near a QSO toward which the number density of HeII decreases rapidly. Zheng & Davisen (1995) show that. taken proximity effect into account. an absorption trough will not generally have a sharp edge at the QSO's redshift. but develop gradually toward shorter wavelengths. Further, Giroux, Fardal & Shull (1995) made a theoretical computation of the

proximity profile of absorption including the contributions of HeII in both the smoothly distributed IGM and the discrete LCs. They found that the absorption profile produced by the diffuse IGM is different from that due to line-blanketing of the LCs especially in the region near to the QSO. Roughly speaking, the edge of the absorption trough due to HeII line blanketing is sharper than that due to the smoothly distributed HeII.

# Chapter 3

# Ionizing Background Radiation Field and Reionization of Intergalactic Medium (IGM)

The density of neutral hydrogen in the diffuse IGM is known to have been extremely low as far back in time as redshift $z \sim 5$. This fact is deduced from the persistent failure to detect G-P HI absorption trough (e.g. Steidel & Sargent 1987). So strong a limit is this, in fact, [e.g. $n_{HI} \leq 10^{-11}$ at $z = 4$ (Webb et al. 1992)], that the density must have been orders of magnitude below that required by the Big Bang nucleosynthesis prediction of light element abundances in the Universe (Walker et al. 1991). This is generally taken to mean that the smoothly distributed fraction of the IGM at $z \sim 5$ and later must have been highly ionized, so that the small residual HI density is undetectable by the G-P test. It implies that there was a ionizing radiation background which ionized the IGM to maintain a small neutral fraction of the IGM. As a natural question, what responses for ionizing background? The most plausible candidate is QSOs. The source of the required metagalactic ionizing flux has been a subject of debate and controversy, as Shapiro & Giroux (1987; see also Dounahue & Shull 1987) have argued that the QSOs detected in optical surveys cannot provide the required number of photons to ionize the medium by $z \geq 3$. The possible complementary sources are unaccounted AGNs, young star-forming galaxies, where high-mass stars produce metals and UV photons (Ostriker & Ikeuchi 1983; Bechtold et al. 1987; Miralda & Ostriker 1990; Madau 1993; Giroux et al. 1994), and decay neu-

trinos (Sciama 1990; 1994a, b). Different kinds of sources have different implications because different kinds of sources have different emissivities and spectral features, and the spectral shape is an important factor for determining the relative fractions of ionization species. For example, Sciama's decay neutrino photons (1994a, b) with the energy just beyond HI limit egde largely differ from the ones of other sources in energy distribution. So, his theory would give a different prediction on relative fractions of ionization species from others and also a different fraction of neutral hydrogen due to a larger magnitude of the intensity of ionizing background beyond HI limit edge.

The reliable value of the intensity of ionizing background is still unknown so far. A somewhat direct estimate of the intensity of the metagalactic flux at the hydrogen Lyman limit, $J_{912} \simeq 10^{-21} erg^{-1}\, cm^{-2} s^{-1} sr^{-1} Hz^{-1}$, is obtained by measuring the decrease in the counted number of LCs induced by the UV radiation field of a QSO in its vicinity, the so-called proximity effect (Murdoch et al. 1986; BDO 1988; Lu, Wolfe, & Turnshek 1991).

Given the emissivity, spectrum, and number density of the source, taken absorption by the IGM into account, the intensity and the shape of the ionizing background can be derived. The usual way to do it is first to obtain an average effective optical depth from the distribution functions of the LCs and the LLSs, under the assumption that they are uniformly distributed. then, using the exponential absorption law without considering recombination radiation, obtain the intensity of the ionizing backgronud. Of course, this optical depth varies with frequency. So after a sufficient absorption, the spectral shape of background radiation should differ from that of the source. The virtual point of the intensity of ionizing background derived in that way is first to fix the neutral atom amount in the IGM, then considering absorption. In the optically thin case, it is available. In the optically thick case, the neutral fraction, optical depth, and intensity of ionizing background depend on each other. Therefore, in principle, the exact calculation of background UV field have to resort to solve the transfer equation and ionization equation simultaneously.

## 3.1 Source of the Ionizing Background Radition Field

There are several types of objects which are believed to produce metagalactic UV field. They could be QSOs, AGNs, young stars, decay neutrinos, IGM emission, and so on.

### 3.1.1 QSOs

Luminous QSOs have long been thought to be major contributors to UV at $z > 2$, owing to their relatively hard spectral energy distributions in the EUV (Ree & Setti 1970; Sargent et al. 1980), despite the fact that they are rare objects. Early estimates were fairly uncertain since the exact form of the QSO luminosity function at $z > 3$ was not well known (e.g. Bechtold et al. 1987). Recently, the situation has greatly improved (see Schneider, Schmidt, & Gunn 1989; Irwin, McMahon, & Hazard 1991; Boyle, Jones, & Shanks 1991; Schneider, Schmidt, & Gunn 1991; Warren, Hewett, & Osmer 1991), and there are now sufficient numbers of QSOs known with $z_{em} = 3-5$ so that the luminosity function for very high redshfit QSOs can be discussed. Using recent luminosity function, Madau (1992) and Meiksin & Madau (1993) have recomputed the QSO contribution to $J_{21}$ and found that $J_{21} \sim 0.1-0.7$. This value is quite closed to that derive from the proximity effect.

### 3.1.2 AGNs

At high redshift, only the bright end of the QSO luminosity function is observed directly, and the contribution of the dimmer, but more numerous AGNs to UV may be important. At low redshfits, the relative importance of the AGNs is even greater, since the high luminosity objects are less common. Fall & Pei (1993) show that a plausible extrapolation of the QSO luminosity function to low luminosity can increase $J_{21}$ by a factor of 2. Furthermore, Terasawa (1992) used accretion disk models for AGNs and showed that low luminosity AGNs make up most of the soft X-ray background and $J_{21} \sim 1$ at $z = 3$.

### 3.1.3 Young Star in Galaxies

Massive, young stars in high-redshfit galaxies may contribute to $J_{21}$ at HI edge even if QSOs dominate at shorter wavelength (Rees & Setti 1970; Tinsley 1972; Code & Welch 1982; Bechtold et al. 1987; Shapiro & Giroux 1989; Songaila, Cowie, & Lilly 1990; Miralde-Escudé & Ostriker 1990; Cen & Ostriker 1993). Miralde-Escudé & Ostriker (1990) have constructed the most detailed models, and show that plausibly $J_{21}$ may be as high as 4 at $z = 3$. and thus exceed the contribution of the QSOs. However, in general, the contribution of young star depends on a lot of factors, such as the initial mass function, the mass cut-off on the high end, the star formation rate as a function of time, the absorption by dust and gas, and so on. Hence the estimates of young star contributions have fairly large uncertainties.

### 3.1.4 Decay Neutrinos

Sciama (1990; 1993; 1994a, b) pointed out that decay neutrinos with a lifetime of $\sim 10^{23}s$ and a energy in the range of $13.6 - 15\,ev$ may produce sufficient UV photons, which can ionize hydrogen, but not helium. The contribution of decay neutrinos to $J_{21}$ may be 10 or more times bigger than that of the QSOs.

Sciama's theory makes testable predictions. If decay neutrinos are also making up the dark matter in local galaxies, then they might produce observable line emission in rich galaxy clusters. Unfortuately, it has not been seen in observations yet (Fabian, Naylor, & Sciama 1991; Davidsen et al. 1991). However, the negative observation might be caused by the absorption of gas in clusters.

### 3.1.5 IGM Emission

A diffuse IGM may produce HeII Ly$\alpha$ $\lambda 304\mathring{A}$ and other line emission which is smeared out with redshfit (Field 1959; Kurt & Sunyaev 1967; Weymann 1967; Jakobsen 1980; Barcons, Fabian, & Rees (1991). If the IGM is photoionized, the recombination HeII $\lambda 304\mathring{A}$ is probably negligible (paresce, McKee, & Bowyer 1980), but if the IGM is collisionally ionized and clumped, then HeII $\lambda 304\mathring{A}$ may be substantial. This last scenario requires substantial kinetic energy input into the IGM, perhaps from shocks (Cen & Ostriker 1994).

## 3.2 Calculation of the Ionizing Background Radiation Field

Estimates of the diffuse UV field have been presented by several authors (Sargent et al. 1980; Carswell 1985; and Bechtold et al. 1987). In order to derive the radiation field from known sources, the continuum absorption by the IGM must be taken into account because it will be significantly modified the UV radiation field. If known averaged emissivity of the ionizing radiation sources and taken the continuum absorption by the IGM into account, the mean intensity of the ionizing radiation is given by

$$J_\nu(\nu_{obs}, Z_{obs}) = \frac{c}{4\pi H_0}\int_{z_{obs}}^{z_{max}} \frac{(1+z_{obs})^3}{(1+z)^3}\frac{\epsilon(\nu,z)exp[-\tau(\nu_{obs},z_{obs},z)]}{(1+z)^2(1+2q_0z)^{0.5}}dz, \quad (3.1)$$

where $\epsilon(\nu,z)$ is the proper volume emissivity of sources at frequency $\nu = \nu_{obs}(1+z)/(1+z_{obs})$ and redshift $z$, and $exp[-\tau(\nu_{obs},z_{obs},z)]$ is the average transmission. The diffuse emission from the IGM is omitted in above equation.

As an example, let us concentrate on the UV background radiation field produced by QSOs. The emissivity of QSOs may be in general written as

$$\epsilon(\nu,z) = \epsilon(\nu^*,0)(1+z)^3\Psi(z)K(\frac{\nu}{\nu_*}). \quad (3.2)$$

Here $K(\frac{\nu}{\nu_*})$ represents the spectral shape, normalized to 1 at a frequency $\nu^*$; $\epsilon(\nu^*,0)$ is the volume emissivity ( $ergs\,s^{-1}cm^{-3}Hz^{-1}$) at $z=0$ and at frequency $\nu^*$; Corresponding to optical surveys, $\nu^*$ is usually taken to be the frequency corresponding to 4400Å, roughly the center of the B-magnitude band. The factor $(1+z)^3$ accounts for the increase in proper emissivity per unit volume that would result if no evolution of sources; $\Psi(z)$ descirbes the evolution of sources.

The $\epsilon(\nu^*,0)$ may be given in terms of the luminosity function.

$$\epsilon(\nu^*,z) = \int_{Lmin}^{\infty}\Phi(L,z)LdL \quad (3.3)$$

where $L_{min}$ is the nimimum luminosity of QSO and $\Phi(L,z)$ is the QSO luminosity function. For instance, adopted a fitted QSO luminosity function

(Madau 1992), which have a a broken power law form in a flat Universe(Boyle 1991),

$$\Phi(L,z) = \frac{\Phi^*}{L^*(z)}[(\frac{L}{L^*(z)})^{3.9} + (\frac{L}{L^*(z)})^{1.5}]^{-1}, \tag{3.4}$$

with

$$L^*(z) = (1+z)^{3.45}, \quad z \leq z_c \tag{3.5}$$

$$L^*(z) = L^*(z_c), \quad z \geq z_c, \tag{3.6}$$

where $z_c = 1.9$ and $z_c$ is the redshfit at which the lumonosity evolution switches off, and assumed $L_{min}$ equals to $0.0017L^*$ corresponding to $M_{B_{max}}(0) = -18$, thus a resultant $\epsilon(\nu^*, 0) = 6.7\times10^{23} h_{50}\, Hz^{-1} Mpc^{-3}$. However, the value of the emissivity depends very much on the QSO luminosity function. In fact. the luminosity function of QSO above $z = 3$ is rather controversial (Irwin et al. 1991; Schmidt, Schneider, & Gunn 1991). This uncertainty results in an uncertainty of emissivity by a factor of 3 giving an uncertainty of intensity of UV background of approximately a factor of 3.

$exp[-\tau(\nu_{obs}, z_{obs}, z)]$ in Eq.(3.1) indicates the absorption by HI, HeI, and HeII as photons travel through the IGM and it depresses the maganitude of metagalactic field and modifies its spectral shape. The absorption by the IGM plays an important role in determining the UV radiation background. To compute UV radiation background, the form of the optical depth as a function of redshift is a key point.

### 3.2.1 Absorption by the Diffuse IGM

The optical depth due to the Lyman continuum absorption of HI, HeI and HeII in the diffuse IGM component for a photon that travels through the Universe in the redshift interval $(z, z+dz)$ can be calculated as

$$\frac{d\tau}{dz} = n(HI)\sigma_{eff}\frac{dl}{dz}, \tag{3.7}$$

where the effective ionization cross section is defined by

$$\sigma_{eff} = \frac{\sigma_{HI}(\nu) + \eta_{HeI}\sigma_{HeI}(\nu) + \eta_{HeII}\sigma_{HeII}(\nu)}{\sigma_{HI}(\nu_{HI})}. \tag{3.8}$$

Here $\eta_{HeII}$ is the ratio of HeII number density to HI number density and $\eta_{HeI}$ is a silimar quantity for HeI. Based on the photoionization equilibrium, it can be written as (Miralda & Ostriker 1992):

$$\eta_{HeII} = \frac{n_{HeII}}{n_{HI}} \sim 1.8 \frac{J_{HI}}{J_{HeII}}. \tag{3.9}$$

More important absorption is produced by H and He in discrete absorbers rather than in diffuse IGM. Becasue the total number density of H or He in absorbers is larger that in the diffuse IGM and further it results, through recombination, in the number density of HI, HeI or HeII in absorberd much larger than that in the diffuse IGM.

### 3.2.2 Absorption by the Clumped IGM

The discrete absorbers including both the LCs and the LLSs make a significant contribution to the opacity of the Universe to ionizing radiation (Bechtold 1987; Shapiro, Giroux & Babul 1989; Miralda & Ostriker 1990; Madau 1992). Considering absorbers with distribution function $\partial^2 \aleph / \partial N_{HI} \partial z$, if they distribute randomly in space, then a mean continuum opacity contributed from them in a given redshift interval $dz$ is given by the following formula

$$\frac{d\tau(\nu, z_{obs}, z)}{dz} = \int_0^\infty \frac{\partial^2 \aleph}{\partial N_{HI} \partial z'} [1 - e^{N_{HI} \sigma_{eff}(\nu')}] \tag{3.10}$$

(Paresce, McKee, & Bowyer 1980). Here $\nu' = \nu(1+z')/(1+z)$, and $\sigma_{eff}$ is effctive ionization cross section defined in Eq.(3.8).

The distribution in HI column density and redshift for absorbers is commonly parameterized by the equation

$$\frac{\partial^2 \aleph}{\partial N_{HI} \partial z} = A(1+z)^\gamma N_{HI}^{-\beta} \tag{3.11}$$

with $\gamma \sim 2.46$ and $\beta \sim 1.5 - 1.8$ for the LCs (e.g. Rauch et al. 1992; Press et al. 1993); $\beta \sim 1.3 - 1.5$ for the LLSs. However, the value of $\gamma$ for the LLSs is currently controvesial (e.g. Sargent et al. 1989; Lanzetta 1991). Using different distribution function, one obtain a different opacity (e.g. Miralda & Ostriker 1990; Madau 1992; Meiksin & Madau 1993).

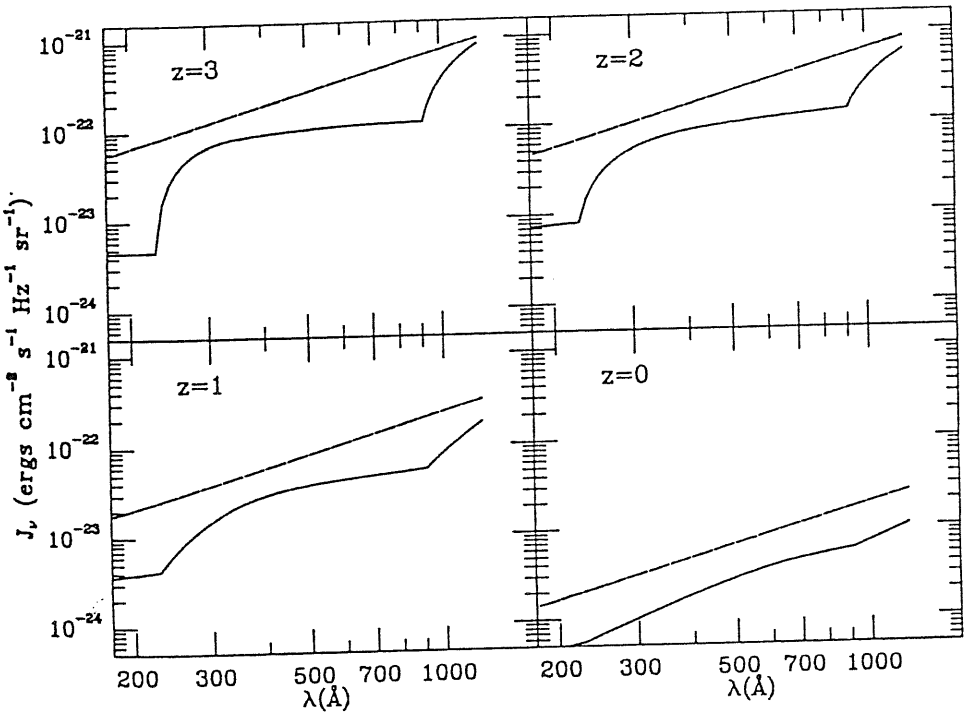


Figure 3.1: Spectrum of a QSO-dominated background at different redshfits for $q_0 = 0.5$ , as modified by the absorption of intervening clouds. Taken from Madau (1992).

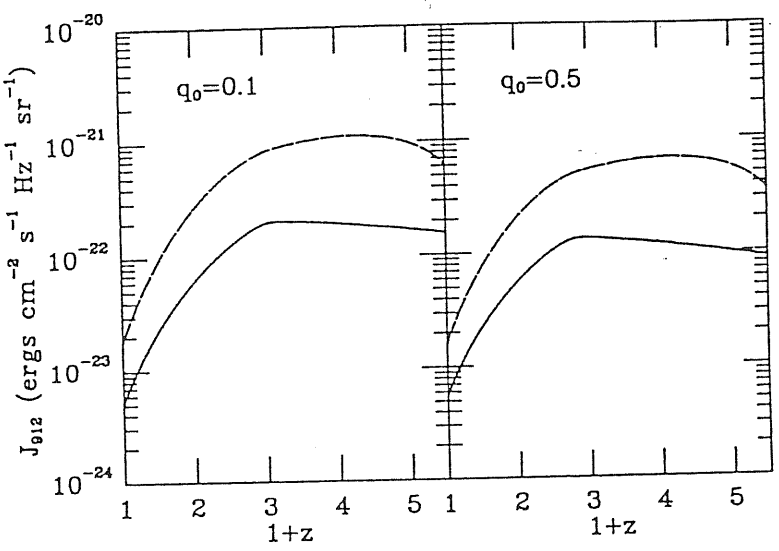


Figure 3.2: Intensity of the diffuse field at 912Å as a function of redshfit for $q_0 = 0.1, 0.5$. The solid line depicts the attenuated flux due to QSOs; the dashed line is derived in the $\tau = 0$ limt. Taken from Madau (1992).

Despite the fact that the primordial abundance of helium in number is about a factor of 12 smaller than the abundace of hydrogen, the absorption by HeII will be extremely important because the recombination coefficient of HeII is $\sim 5.5$ times larger than that of HI, and the intensity at the ionization edge of HeII will in general be smaller than the intensity at the ionization edge of HI. As seen from Eq.(3.9), the quantity $\eta_{HeII}$ will in general be quite large if the spectrum of ionizing field is not very flat. In particular, if the source are dominated by QSOs with a power-law spectral index $\sim 1.4$, then $\eta_{HeII} \simeq 13$ (Miralda & Ostriker 1990), and if the sources are dominated by galaxies or decay neutrinos (Sciama 1994), then the onizing field is fairly soft and so $\eta_{HeII}$ will be even larger.

Since the opacity is a function of the background field $J$, to derive the optical depth, one must solve above equations by iteration. In fact, in previous work (e.g. Miralda & Ostriker 1990), the intensity of the ionizing field is derived by first fixing the amount of HI, HeI and HeII, then taking absorption into account. In this way, one obtains a new ionizing field. Based on photoionization equilibrium, one gets a new value of the amount of HI, HeI

and HeII, then iterate the same procedure, one obtains a new ionizing field again. Do iterations until a converge occurs. Finally, the reliable ionizing field is obtained. Fortunately, the converge process is quite fast.

More recently, Giroux & Shapiro (1994) carried out a detailed calculation in a self-consistent way. Two prominent features of their paper are completeness and self-consistence.

## 3.3 Evolution of the IGM

From the Gunn-Peterson test of HI (e.g. Steidel & Sargent 1987; Cristiani et al. 1995b), we know that the IGM was in a highly ionized stats after the epoch $z \sim 5$. On the other hand, the Universe is neutral after the epoch of recombination (occurred at $z \sim 10^3$) accoring to standard Big Bang cosmology. Both facts indicate that the Universe must have experienced a reionization epoch some time between $z \sim 10^3$ and $z \sim 5$.

Once a ionizing source appears, the UV photons from it will ionize its surrounding medium. Because of the expansion of the Universe, the number density gets small with increasing time. This fact results in a expanding ionized region surrounding the ionizing source. The individual ionized regions will overlap at a certain time, say $z_{ov}$. Before $z_{ov}$, there are unionized patches in the Universe; After $z_{ov}$, the Universe was fully ionized. In order to satisfy the G-P constraint at a redshfit, say $z = z_{GP}$, the necessary condition is $z_{ov} > z_{GP}$ (Shapiro & Giroux 1987; Donahue & Shull 1987; Meiksin & Madau 1993).

The history of evolution of the diffuse IGM may be divided into two parts. One is called reionizing epoch, the other is called fully ionized epoch. The main reason to do it is that the physical processes in reionizing epoch differs from that in fully ionized epoch.

### 3.3.1 Reionizing Epoch

Studying of the problem of an ionization region expanding away from a single ionizing source in an expanding Universe is similar to that for an H II region around an O-star embedded in the interstellar medium (ISM) (Strömgren 1939). However a new character in the IGM arises from Hubble expansion.

Because of a decrease of number density with increasing time, the ionization front in the diffuse IGM is expansive instead of steady in the ISM.

Let $S(r,t)$ be the number of ionizing photons emitted by the central source which pass through a sphere of comoving radius $r$ per second and $a(t) = (1+z_i)/(1+z)$, where $z_i$ is the redshift at which the source turns on. Based on the equation of ionization equilibrium and the equation of radiative transfer, the outgoing photon flux (Shapiro & Giroux 1987; Donahue & Shull 1987; Meiksin & Madau 1993) is given by

$$\frac{\partial S}{\partial r} = -4\pi r^2 a^{-3} n_{H,i}^2 c_l \chi^2 \alpha_B, \tag{3.12}$$

where $n_{H,i}$ is the average intergalactic H atom number density at $z_I$, the gas clumping factor $c_l = < n_{H,l}^2 >^{1/2} / n_H$, where $n_{H,l}$ is the local number density ($c_l = 1$ for a uniform IGM), $\chi$ is the ionized fraction $\sim 1$ throughout the interior of the HII region, and $\alpha_B$ is the recombination coefficient to levels $n \geq 2$. Integrating Eq.(3.12), the rate $S(r)$ of ionizing photons at distance from the source is given by

$$S(r) = S(0) - \frac{4}{3}\pi r^3 a^{-3} n_{H,i}^2 c_l \chi^2 \alpha_B \tag{3.13}$$

inside the HII region. A simple, but not bad, way to consider the presence of He atoms is replacing one of the powers of $\chi = 1$ above by $\chi_{eff} = 1 + pf(He)$, where $p = 0, 1$, or 3 according to whether He is mostly HeI, HeII, or He III, respectively, inside the HII region, and $f(He) \sim 0.08$ is the helium abundance by number relative to hydrogen.

The actual HII region expands bounded by an ionization front defined as the surface across which the outgoing ionizing photon flux is balance by the incoming neutral particle flux. This balance is expressed as a continuity condition in the frame of the front given by

$$4\pi r_I^2 n_H (\frac{dr_I}{dt} - H r_I) = S(0) - \frac{4}{3}\pi r^3 a^{-3} n_{H,i}^2 c_l \chi^2 \alpha_B, \tag{3.14}$$

where $r_I$ is the proper radaus of the ionization front. $H$ is the Hubble constant, $S(0)$ is the number of ionizing photons emitted from the central source per unit time.

The condition that a uniformly distributed point sources with number density $n_s$ fully photoionize the IGM is that their individual ionized regions

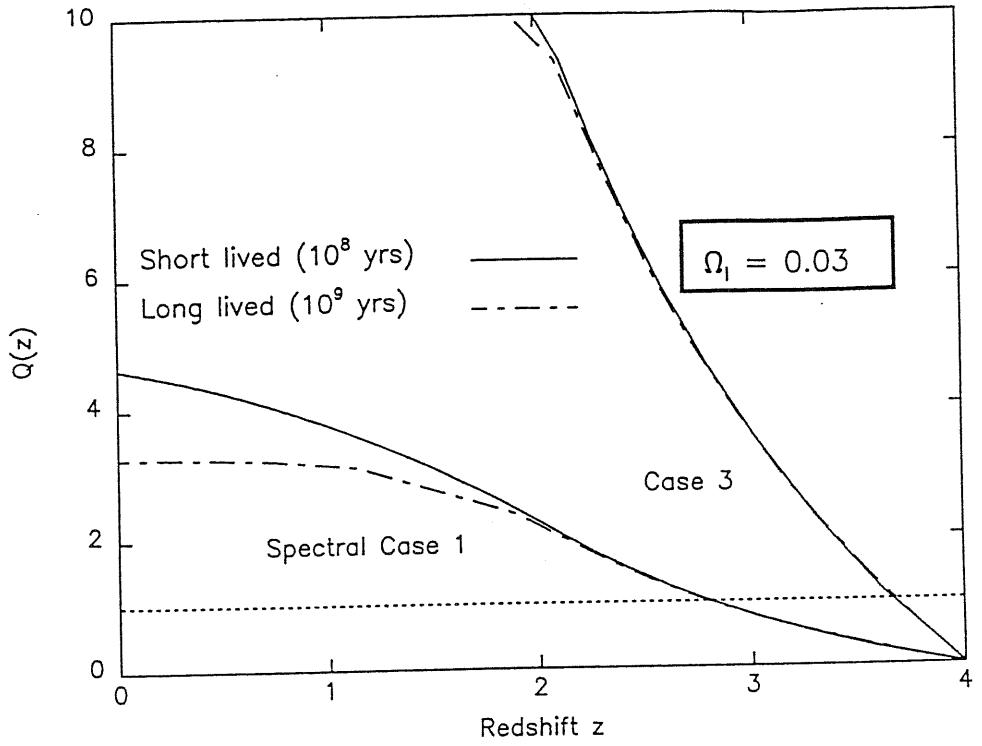


Figure 3.3: Porosity as a function of redshfit. For the soft spectrum and the luminosity function of Weedman (1986) (case 1), the IGM is not ionized until $z \approx 2.8$. Taken from Donahue & Shull (1987)

overlaping and is given by

$$Q(z) = \frac{4}{3}\pi r_I(z)^3 a^3(z) n_s(z) = 1, \tag{3.15}$$

where $Q$ is called porosity parameter, which equals to the fractional volume filling factor of ionized gas before overlaping.

Shapiro & Giroux (1987) and Donahue & Shull (1987) showed that the QSOs are insufficient to provide enough ionizing photons which ionize the IGM to the point avoiding the G-P effect unless other kinds of abundant sources of ionizing radiation existed as early as $z > 3.5$, or something else occured, such as shock waves from explosive galaxy formation or pancake collapse or both, heats the IGM at $\geq 3.5$ to temperatures $T \geq 10^6 K$.

However, in fact, the luminosity functions of QSOs at $z > 3$ are rather uncertain (see e.g. Ostriker & Heisler 1984 Boyle, Jones, & Shanks 1991; Hewett, Foltz, & Chaffee 1993) because high redshift QSOs are fainter. In addition, obscuration by dust in damped Ly$\alpha$ systems results in $10\% - 70\%$ of the bright QSOs at $z = 3.4$ missed from optical samples. It helps to account for the UV background radiation to satisfy the G-P constraint. At present. there exists an uncertainty of a factor of $\sim 3$ in the counts of QSOs at $z \sim 3$ (Schmidt et al. 1991; Boyle 1991). If we agree that a considerable fraction of high redshfit QSOs is missed in current surveys, the required amount of ionizing photons may be provided only by QSOs (Meiksin & Madau 1993).

### 3.3.2 Evolution of the IGM after Overlaping

Given the cosmological density of the IGM, the emissivity of ionizing radiation as a function of frequency and redshift, and the absorption by various objects in the Universe, we can calculate the evolution of the fraction of each ionized state of hydrogen and helium, and the temperature of the IGM. The fundamental method for studing an evolution of the IGM is based on the equations of ionization equilibrium and thermal equilibrium.

#### a. the Equation of Ionization Equilibrium

In general, the equation of photoionization equilibrium for any two successive stages of ionization $i$ and $i+1$ of any element $X$ may be written

$$4\pi n^{X(i)} \int_{\nu_i}^{\infty} \frac{J_\nu}{h\nu} \sigma_\nu X(i) d\nu = n_e n^{X(i+1)} \alpha_A(X(i), T), \tag{3.16}$$

where $J_\nu$ is the mean intensity of radiation; $n^{X(i)}$ and $n^{X(i)}$ are the number densities of the two successive stages of ionization; $\sigma_\nu X(i)$ is the photoionization cross section from the ground level of $X(i)$ with the threshold $\nu_i$; $\alpha_A(X(i), T)$ is the recombination coefficient of the ground level of $X(i+1)$ to all levels of $X(i)$. The left-hand side of above equation gives the number of photoionizations per unit volume per unit time and the right-hand side of above equation represents the number of recombinations per unit volume and per unit time.

In the case in which collisional ionization plays an important role, the

ionization equation becomes

$$4\pi n^{X(i)} \int_{\nu_i}^{\infty} \frac{J_\nu}{h\nu} \sigma_\nu X(i) d\nu + n_e n^{X(i)} \gamma^{X(i)} = n_e n^{X(i+1)} \alpha_A(X(i), T), \quad (3.17)$$

where $\gamma^{X(i)}$ is a collision ionization rate coefficient.

**b. Equation of Thermal Equilibrium**

The temperature of the IGM is fixed by the equilibrium between heating-ing and cooling.

$$\Gamma = \Lambda, \quad (3.18)$$

where $\Gamma$ it the heating rate and $\Lambda$ is the cooling rate.

**♣Heating Processes**

1. Heating by Photoionization

   When a photon of energy $h\nu$ is absorbed and causes an ionization. the photoelectron produced has an initial energy $\frac{1}{2}mv^2 = h(\nu - \nu_0)$. where $\nu_0$ is the threshold of ionization energy. The heating rate of photoionization in unit $erg\, cm^{-3} s^{-1}$ is

   $$\Gamma_{photo} = 4\pi n_{HI} \int_{\nu_{HI}}^{\infty} \frac{J_\nu}{h\nu} h(\nu - \nu_0) \sigma_{HI} d\nu. \quad (3.19)$$

   It is a major source of heating.

2. Heating by Shocks

   Ikeuchi and Ostriker(1986) introduced shock heating into heating processes of the IGM. They pointed out that some pregalactic objects exploded at the early epoch $z \sim 5 - 20$ and produced a shock. This shock would propagated over the Universe. As the shock pass through gas clouds. it injects energy into gas. A portion of this energy converts to increase gas temperature as a heating source. $\Gamma_{shock}$ is proportional to the product of the number density of shock source. the efficiency of energy liberation and the fraction of liberated energy converted as thermal energy. The shock-heating rate is given in the paper of Ikeuchi & Ostriker (1986).

The total heating rate $\Gamma$ is contributed by both those heating processes,

$$\Gamma = \Gamma_{photon} + \Gamma_{shock}. \tag{3.20}$$

We should mention here that there is a third heating source by cosmic rays (Stebbins & Silk 1986; Nath & Biermann 1993).

♣ **The cooling processes:**

1. Recombination

   In each recombination, a thermal electron with energy $\frac{1}{2}mv^2$ disappears. we assume that thermal electrons velocity has an Gaussian distribution because the time scale of thermalization is much shorter than Hubble scale. By averageing this quantity over all recombination, one may obtain a cooling rate of recombination. It is a major cooling source.

2. Collisional Ionization and Excitation

   When electrons collide with atoms or ions and cause them ionizing or excitation, electrons lose their thermal energy. It is one of the cooling processes. In the low density case, it is not important. For our interest. it can be neglected.

3. Free-Free Radiation

   As an electron moves around an ion, the electron emits free-free radiation and loses a portion of its thermal energy. For our case, it is one of the important cooling processes.

4. Inverse Compton Scattering

   While electrons scatter with the cosmic microwave background (CMBR) photons, because the energies of CMBR photons are very low, a very small portion of the thermal energies of electrons will be converted to photons in the process of collision. Due to a high number density of CMBR photons, this cooling process can not omitted, especially for the early epoch.

5. Expansion

   If a cloud is bounded by an external pressure, as a cloud expands, it has to provide some energy against the external pressure. The lost of energy causes cooling.

Expressions for cooling rates of those processes are summarized in the papers by Sherman (1980), Black (1981), Stebbins & Silk (1986), and Collin (1991). The total cooling rate $\Lambda$ includes all contribution from all cooling processes. In different situations, the dominated cooling process besides recombination is different.

In above thermal equilibrium equation, all contributions from all species of elements should be included. For instance, helium plays an important role in determining the temperature of the IGM, because the mean thermal energy of photoelectrons ionized from helium is greater than that from hydrogen.

In previous works (e.g. Black 1981; Ikeuchi & Ostriker 1986), it is usually assumed that the IGM is in ionization and thermal equilibrium. There are two main reasons for making the thermal equilibrium assumption. One is for simplicity, the other is that the observational data at that time are not rich enough to require more accurate treatment. The gas is generally in ionization equilibrium, since the expected intensity of the ionizing background is high enough to make the ionization time-scale much shorter than Hubble time. However, in fact, the assumption of thermal equilibrium is not good enough for studying the IGM, basically because the recombination time in the IGM is longer than the Hubble time for $z \leq 10$, especially for low density case (Giallongo & Petitjean 1994). In other words, there is no sufficient time to reach thermal equilibrium. We may expect that shortly after the gas is fully ionized, the temperature of gas reached maximum, then the temperature decreased due to cooling. Because the cooling time scale is longer the Hubble time, the temperature remains somewhat higher than the equilibrium temperature. Naturally, one way to more precisely deal with this problem is to solve the evolution equation of temperature with time (Meiksin 1994; Miralda and Rees 1994). The cost is increasing the complication. Their studies show that the temperature is indeed dependent on the initial condition and the properties of ionizing source, e.g. the luminosity, the shape of spectrum and so on.

# Chapter 4

# Ly$\alpha$ Clouds (LCs)

Since the discovery and correct identification of the Ly$\alpha$ forest by Lynds (1971) over two decades ago, it has been recognized that these ubiquitous features in the spectra of high redshfit QSOs held enormous potential for the study of the nature and evolution of the IGM as well as the development of structure in the Universe at the low end of the mass spectrum. The last decade, especially recent years, was a period of very rapid advancement in our knowledge and understanding of the IGM, both in its smooth and clumped form. We will summarize the essential observational facts about the LCs below. It is important to realize the status of these observations since they are to be compared with the models and theories.

## 4.1 HI Equivalent Width Distribution

A fundamental observational feature of the LCs, first noted by Sargent et al. (SYBT, 1980), is that their equivalent widths $W$ are exponentially distributed. The number of lines in a QSO spectrum depends on the limiting equivalent width $W_{lim}$ in the rest frame. Murdoch et al. (MHPB, 1986) used a compilation of data and derived a fitting formula of equivalent width distribution between $0.2 < W < 1.6\mathring{A}$

$$\frac{d\aleph}{dW} = (\frac{\aleph^*}{W^*})e^{-\frac{W}{W^*}} \tag{4.1}$$

with $W^* = 0.362 \pm 0.021\mathring{A}$ and $\aleph^* = 154 \pm 11$, where $W^*$ is independent of redshift $z$. The value of the characteristic rest frame wavelength $W^*$ is found

to be in the range from about 0.25Å to 0.40Å (SYBT; Young, Sargent, & Boksenberg 1982; MHPB). This formula becomes poorer as weaker lines are included. In the region of $W \leq 0.2$, the distinct departure of the data from a pure exponential distribution appears. Press et al.(1993) fitted the data for $W < 0.2$Å and got a power law distribution with the index of power -1.5 in this small $W$ region.

Jenkins (1991) and Barcons & Webb (1991) pointed out that the value $W^*$ in the range $0.25 - 0.35$Å derived from the rest equivalent width limited samples is inconsistent with the power law index $\beta$ being in the range $\sim 1.5 - 1.9$.

## 4.2 HI Column Density Distribution

Usually the column density distribution is approximately as a power law

$$\frac{d\aleph}{dN} \propto N^{-\beta} dN, \tag{4.2}$$

first established by Carswell et al. (1984). Hunstead et al. (1987a, 1988) obtain $\beta = 1.57 \pm 0.05$ fitting to a range $13.25 < logN < 16$, and find that a single power law is a good fit. This contrasts with Carswell et al. (1987), who found evidence of a break at $logN \sim 14.35$. Petitjean et al. (1992) report $\beta = 1.49 \pm 0.02$ as the best single power law fit over the range $13.7 < logN < 21.8$. However, they obtain a somewhat steeper value $\beta = 1.83 \pm 0.06$ for a fit restricted to $13.7 < logN < 16$. More recently, Press et al. (1993) reported that a single power low with $\beta = 1.43 \pm 0.04$ may fit the data well. This year Cristiani et al. (1995a) claimed that the column density distribution of the LCs may be well fitted by a power-law with a break or cutoff at $logN \sim 14.5$ and a featureless power-law distribution is rejected with a probability of 99.94%.

There is a lively debate on the value of $\beta$ as $N$ varies over 10 orders of magnitude, from $10^{12} - 10^{22}\, cm^{-2}$ (see, e.g. Tytler 1987; Bechtold 1988; Carswell et al. 1987; Hunstead 1987a, 1988; Rauch et al. 1992; Petitjean et al. 1993; Press et al. 1993). Theoratically, an unbroken power law of column density distribution over 9 decades was shaken by the question: why is there no feature in the distribution for $N_{HI} \geq 10^{17}\, cm^{-2}$? At such column densities clouds become optically thick and should form a (nearly) neutral core. The

presence of a neutral core should complicate the observational picture and produce a feature on column density distribution around $N_{HI} \geq 10^{17}\, cm^{-2}$. Data published by Bechtold (1988) seemed to show a break, confirming the theory of optically thick clouds. However, subsequent work by Sargent et al. (1989) showed no break, reaffirming Tytler's (1987) earlier study. Part of the problem is that the range of $N_{HI}$ of interest corresponds to a saturated part of the curve of growth. Therefore, the determination of column densities in this region is quite uncertain and make comparison of theory and observations ambiguous.

## 4.3 Evolution of Number Density with Redshift

After years of study since the LCs were discovered (Lynds 1971), the evolution of the number of the LCs per unit redshfit has been established as following a power law

$$\frac{d\aleph}{dz} = (\frac{d\aleph}{dz})_0(1+z)^{\gamma}. \tag{4.3}$$

The main effort has been concentrated on determining the value of the evolution parameter $\gamma$.

The first evidence for evolution in Ly-$\alpha$ line density was presented by Peterson (1978), based on a preliminary study of four QSOs. For clouds of cross-section $\sigma$ and number density $\rho_o$ per unit co-moving volume, he showed that the corresponding number density of absorption lines per unit redshift is given by

$$\frac{d\aleph}{dz} = \sigma\rho_0\frac{c}{H_0}(1+z)(1+2q_0z)^{-0.5}. \tag{4.4}$$

For a non-evolving cloud population, $\sigma\rho_0$ is constant and $d\aleph/dz$ then depends weakly on redshift, $\gamma = 1$ for $q_0 = 0$ and $\gamma = 1/2$ for $q_0 = 1$. $\gamma$ significantly greater than 1 indicates the strong evolution in the number density of the LCs.

For a long time the value of $\gamma$ was a subject of controversy, with different observers determining (from different data set) values as disparate as $\gamma = -2.1$ and $\gamma = 2.36$. We want to mention that a part of the problem was caused by the proximity effect, which will be discussed later.

**Table 6.1. Estimates of $\gamma$**
(compiled from the literature)

| Reference | $\gamma$ |
|---|---|
| Peterson (1978) | Evolution ($\gamma \geq 1$) |
| Eills (1978) | No Evolution |
| Sargent et al. (1980) | $0.48 \pm 0.54$ |
| Weymann et al. (1981) | 2.5 |
| Zou et al. (1982) | No Evolution |
| Young et al. (1982) | $1.81 \pm 0.48$ |
| Carswell et al. (1982) | $1.4 \pm 0.7$ |
| | $0.6 \pm 0.6$ |
| | $-2.1 \pm 1.5$ |
| Peterson (1983a) | $2.2 \pm 0.4$ |
| Peterson (1983b) | $2.36 \pm 0.36$ |
| Phillipps & Ellis (1983) | $-0.4 \pm 0.3$ |
| Sargent & Boksenberg (1983) | 2.1 |
| Atwood et al. (1985) | $1.7 \pm 1.0$ |
| Lu et al. (1991) | $2.75 \pm 0.29$ |
| Bahcall et al. (1993) | $1.26 \pm 0.13$ |
| Bechtold (1994) | $1.89 \pm 0.28$ |
| Boksenberg (1995) | $0.58 \pm 0.50$ |

The value of $\gamma$ recently obtained by Press et al.(1993) for lines with rest equivalent width $W > 0.32$ Å, corresponding to $N_{HI} > 1.6 \times 10^{14} cm^{-2}$, is 2.46. This result is close to Lu et al's and Rauch et al's(1992). Bechtold (1994) reported that $\gamma = 1.89 \pm 0.28$ for lines with equivalent width greater than $0.32\mathring{A}$ and $\gamma = 1.32 \pm 0.24$ for lines stringer than $0.16\mathring{A}$. There is a significant trend of decreasing $\gamma$ with decreasing equivalent width limit. By combining with HST results for low-redshift clouds (Bahcall et al. 1993a), a single $\gamma$ is an acceptable fit to data, with $\gamma = 1.26 \pm 0.13$ for $z = 0 - 4.1$. although an inflection at $z \sim 1.5$ exists. If only strong lines are included. there is no significant inflection.

The satisfaction in achieving agreement between different observers was undermined however by recent determinations of $\gamma$ values as divergent as $\gamma = 2.75 \pm 0.29$ (Lu et al. 1991) from a compilation of 38 QSOs and $\gamma = 1.89 \pm 0.28$ (Bechtold 1994) from a homogeneous sample of 34 QSOs. Both results were for strong lines frame equivalent widths exceeding $W = 0.32\mathring{A}$. Bechtold found an even more disturbing result from a sample of line complete to $W = 0.16\mathring{A}$ in her 34 QSO spectra. This sample yielded $\gamma = 1.32 \pm 0.24$. a striking result consistent with almost no evolution.

A power-law extrapolation (4.3) with Bechtold's small value of $\gamma$ predicts more absorbers at $z \sim 0$ than previously thought, consistent with results from the HST (Morris et al. 1991; Bahcall et al. 1991, 1992;). HST data for 3C273 ($z_{em} = 0.158$) and H1821+643 ($z_{em} = 0.297$) indicate $d\mathcal{N}/dz \sim 13 \pm 5$ lines per unit redshfit at $z \sim 0$. The value $\gamma = 1.89$ predicts a density at $z \sim 0$ only $\sim 1\sigma$ lower than observed.

## 4.4 Temperatures of the LCs

The width of the absorption lines is caused by the Doppler effect of velocities of the individual ions causing the absorption, due to gas temperature and bulk motions. Most lines are narrow with widths less than 1Å, corresponding to a velocity dispersion in the range $\leq 50\, kms^{-1}$. Rauch et al.(1992) obtained a median value of HI velocity $b = 35\, kms^{-1}$. It is still not very clear whether the velocity measured is a result of thermal velocity or of the combination with bulk motion. In other words, which factor of them dominates line broadening. One way to determine it is by measuring the Doppler widths of other elements simultaneously. for instance, $b_{HeII}$. In the case of pure thermal

broadening, $b_{HeII} = 0.5 b_{HI}$, while in the case of bulk motion broadening, $b_{HeII} = b_{HI}$. Another open question related to the Doppler width of the absorption lines is whether the broader lines come from bulk motion or contamination by line-blending. The only way to distinguish them is to resort high resolution. The observational situation is unfortunately controversial at the moment. Early measurements of the width of the Ly$\alpha$ lines had indicated a temperature close to $5 \times 10^4 K$ (corresponding to $b \sim 30\, kms^{-1}$). More recently echelle data at $10\, kms^{-1}$ resolution reveal a large fraction of narrow lines with $b < 20\, kms^{-1}$ (Pettini et al. 1990; Hunstead & Pettini 1991). Even excluding lines with $b < 10\, kms^{-1}$, which could be either spurious because of the limit $S/N$ ratio of the data or unidentified metal lines, the fraction of lines with $10 < b < 20\, kms^{-1}$ is $\sim 15 - 20\%$, corresponding to the temperature in the range $\sim 6500 - 26000 K$. If this is a real situation, such low temperature of gas is hard to explain.

As pointed out by Pettini et al. (PHSM, 1990a), low temperature can be obtained by increasing the gas density, and hence increasing cooling rate. However, the derived number density, which give the observed low temperature, for typical clouds is $\sim 1\, cm^{-3}$. Consequently, the cloud sizes are $\sim 1 kpc$. This value is too small to coincide with the observed low limit of clouds size $\sim 90 h^{-1} kpc$ (Bechtold et al. 1994). An alternative solution to the problem of explaining low temperatures can be obtained allowing for adiabatic cooling due to cloud expansion against the external pressure of a diffuse intergalactic medium (Giallongo & Petitjean 1994). On the other hand, instead increasing cooling, one expects that decreasing heating rate may also depress the temperatures. Indeed, Sciama's decay neutrino theory (1990, 1994a, b) can produce the required low temperature if metagalactic UV radiation field is not very hard so that the heating produced by ionizing HeI and HeII is negligible.

This low temperature reported by Pettini et al. (1990) was challenged by Carswell et al.(1991) who maintained that the higher value of the temperature is the correct one. The controversy involves difficult questions of data analysis and has been discussed by Peacock (1991). Further contributions have been made by Donahue and Shull (1991) and Rauch et al. (1993). Their re-analysis shows that there is little evidence for a significant population of cool clouds with Dopper parameters less than about $15\, kms^{-1}$. The considerable fraction of cool clouds with $b < 20\, kms^{-1}$, reported by PHSM is probably a bogus effect of low $S/N$ ratio.

PHSM also found a strong $b - N_{HI}$ correlation, which can be described by a simple fit (Bajtlik & Duncan 1991),

$$b = [11 + 14(logN_{HI} - 13)]\, kms^{-1}. \tag{4.5}$$

A disturbing fact is observations of Q1100-264 ($z_{em} = 2.14, B = 16.0$) by Carswell et al. (1991) and of Q0000-263 ($z_{em} = 4.11, m_r = 17.5$) by D'Odorico, Molaro, & Savaglio (1991) showed no $b - N_{HI}$ correlation. For a brief summary of this controversy see Webb & Carswell (1991), Hunstead (1991) and D'Odorico, Molaro, & Savaglio (1991).

More recently, Tytler (1995) reported that most clouds have velocity dispersions between 22 and $36\, kms^{-1}$ and there is no correlation between velocity dispersion and column density, but some clouds are apparently very cold.

## 4.5 Size of the LCs

We have little direct information on the sizes or shapes of the LCs, but in some cases the same lines are in the spectra of QSOs adjacent in the sky, giving minimum or maximum sizes. Spectral observations of gravitationally lensed QSO, or QSO pair with small projected separation, are a key to understand the size of the LCs. By measuring how many Ly$\alpha$ lines are common in the two component spectra, and equivalent widths of these common lines compare, one can constrain the size of the LCs. An upper limit on the cloud sizes $R < 400h^{-1}kpc$ has been given by Shaver & Robertson (1983) in the pair Q0307-195. On the other hand, Foltz et al. (1984) derived a lower limit to the transverse sizes in the range $5 - 25h^{-1}kpc$ at $z \sim 2$ from the gravitationally lensed pair Q2345+0007. Studies of QSO pairs with large separation(1 arcmin or larger) have detect very few common absorption line, placing upper limits on the $LC$absorber size of 0.5-$2h^{-1}Mpc$. Gravitational lenses have been used to probe much smaller scales.(Smette et al. 1992). These authors found that virtually all of the verifiable Ly$\alpha$ line in one spectra are present in the other, and the equivalent widths of these common linear statistic equal. indicating a firm lower limit of cloud sizes $6kpc$. Unfortunately, the two lensed images are separated by only $\theta = 2".2$, too close to provide a strong upper limit on cloud sizes.

Recently, Bechtold et al.(1994), used the spectra of Q 1343+266 AB, a pair of QSOs at z=2.03 with a projected separation of 9.5 arcsecs, found that the LC radius at $z \sim 1.8$ lies in the range $40h^{-1}Kpc < R < 280h^{-1}Kpc$ with 98% confidence. The median value of R is $90h^{-1}Kpc$.

More recently, Smette et al.(1995) reported that physical extent of the LCs exceeds $100kpc$. An even larger value has been measured by Dinshaw et al.(1995). They used ultraviolet spectra of the QSO pair 0107-025AB ($z_{em} = 0.956, 0.952$) taken with the FOS on the HST and showed that the characteristic transverse size of the LCs is at least $320h^{-1}Kpc$ in the redshfit range $0.5 \leq z \leq 0.9$, larger by nearly an order of magnitude than the best lower limits for the higher redshift LCs determined from the ground. Maximum likelihood gives a most probable diameter of $700h^{-1}Kpc$.

These recent results cannot matched with the pictures of pressure equilibrium and virialization. For instance, if the LCs with such large size are well gravitational confined, the Press-Schechter theory show that their column density should be equal to or larger than $10^{17}\,cm^{-2}$ (Mo, Miralda-Escudé & Rees 1993). So the LCs with such large size and low column densities should not be completely gravity-confined.

## 4.6 Spatial Distributions of the LCs

Previous studies have revealed a practically uniform velocity distribution on the scales larger than $\sim 300\,kms^{-1}$ (see SYBT 1980; Crotts 1989; Barcons & Webb 1991; Rauch et al. 1992). Meanwhile, there were some indications that Ly$\alpha$ lines cluster on smaller scales for equivalent-width-limited samples with a relatively large cutoff equivalent width ($w > w_c = 0.36\mathring{A}$) (Webb 1987; Ostriker et al. 1988; Barcons 1991; Barcons & Webb 1991). Rauch et al.(1992,1993) investigated the clustering properties of the LCs using high-resulotion spectra of two QSOs (0041+813, z=3.38 and 2206-199, z=2.56), the results are rather controversial. In the first case, no evidence for clustering on any scales was found in whole Ly$\alpha$ line sample (295 lines in total). In the second case, a similar sample (101 lines) revealed marginal evidence for clouds clustering at small scales ($50 - 150\,kms^{-1}$). However, this discrepancy can be explained by assuming that clustering properties of the LCs depend on their HI column density (and, hence, their rest-frame equivalent width). The much recent work (Elowitz et al. 1995; Chernomordik 1995; Cristiani

et al. 1995a) seem to confirm the viewpoint of Crotts (1989): "*a gradual progression in clustering strength from virtually no clustering for weak lines to strong-line clustering*".

For studying the clustering problem, the two-point correlation function is frequently used. The velocity difference can be deduced from the redshift difference on not very large scale (SYBT 1980)

$$\Delta v = \frac{c(z_2 - z_1)}{1 + (z_1 + z_2)/2}, \tag{4.6}$$

where $\Delta v$ is the velocity of one cloud as measured by an observer in the rest-frame of thr other. The two-point correlation function in velocity space is defined as (Peebles 1980)

$$\xi(\Delta v) = \frac{N_{obs}(v, \Delta v)}{N_{exp}(v, \Delta v)} - 1 \tag{4.7}$$

where $N_{obs}$ is the observed number of line pairs with velocity of $v - v + \Delta v$ and $N_{exp}$ is the number of pairs expected from a random distribution in redshift. The correlation among the LCs on small scales is much less pronounced than that observed in metal absorption systems.

The weak clustering of the LCs on small scales is expected either in the shocked-shell model (Chernomordik & Ozernoy 1983a; Ikeuchi et al. 1983) or in the gravitational instability model (Rees 1988 and so on). However, it is worth noting that a decrease in clustering with increasing redshift if the gravitation dominates the clouds evolution, or an increase in clustering with increasing redshift for shocked-shell model (Crotts 1987, 1989; Ostriker et al. 1988).

An alternative approach to search for structure of the LCs was firstly adopted by Ostriker, Bajtlik, & Duncan (1988), is studying for large scale voids in the LCs. It is helpful for testing theoretical models concerning the large scale structure in the Universe. Ostriker et al. (1988) found a significant departure from Poisson statistics in distribution of voids in the LCs (but see Webb & Barcons 1991). Since then, several authors have reported that there are megaparsec-size voids in the LCs. A void with comoving size $\sim 23 Mpc$ has been detected by Dobrzycki & Bechtold (1991). However, the observed voids in the LCs could not represent the true distribution of total matter in the LCs, but could arise from the changes in the ionization of the IGM due to fluctuations in the ionizing UV flux (Dobrzycki & Bechtold 1991).

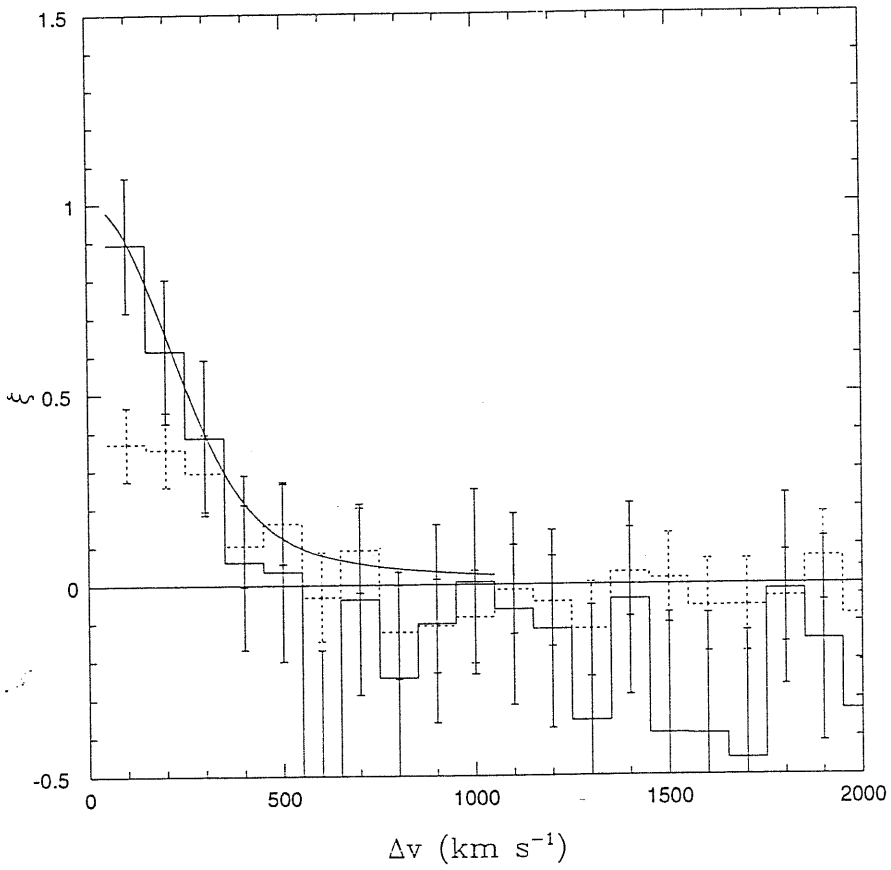


Figure 4.1: Two-point correlation function for the Ly$\alpha$ lines in Q0055-269. The continuous histogram is for lines with $\log N_{HI} \geq 13.8$; the dotted histogram is for lines with $\log N_{HI} \geq 13.3$. The continuous curve is the fitted one. Taken from Cristiani (1995a).

The absent or weak clustering of the LCs on large scales has led to the longstanding belief that the LCs are not associated with galaxies (SYBT). At low redshift, similar absorption lines have been discovered using the HST (Bachall et al. 1991, 1992, 1993a; Morris et al. 1991). This raises the possibility of more-detailed study of the absorber's environment. Bachall et al. (1992, 1993a, b) showed that there are some definite coincidences between the LCs and galaxies along the sightline to the QSO. Morris et al. (1993) showed that the absorbers were not distributed at random with respect to galaxies, but also that the correlation between the LCs and galaxies was significantly weaker than that between galaxies and galaxies. This then raises the idea that some of low-redshift LCs may be associated with galaxies.

More recently, it was reported that at $z \leq 1$ the LCs are physically associated with the corresponding galaxies and the fraction of the LCs which arise in galaxies is more than 20% (Mo & Morris 1994; Lanzetta et al. 1994). This new result runs contrary to, at least at low redshifts, the viewpoint that the LCs are cosmologically distributed, in the Universe (SYBT).

## 4.7 Metallicity of the LCs

The determination of the metal element abundances in the LCs is an important test of their origin. Despite of a number of studies (Norris, Hariwick, & Peterson 1983; Chaffee et al. 1985; Chaffee et al. 1986; Meyer & York 1987; Williger et al. 1989; Lu 1991; Cowie et al. 1995; Savaglio & Webb 1995), our knowledge about the chemical abundance of LCs is still poor. Experimentally determining the metallicity of weak members of the LCs has been a very difficult problem until now because of the limited sensitivity of spectroscopic observations. For example, for a cloud with $logN_{HI} = 13$, $HI/H \sim 10^{-4}$ and $CIV/C \sim 0.2$ (predicted by photoionization models), the stronger member of the CIV doublet at 1548Å will have a rest frame equivalent width of $33m\AA$ if the abundance are solar. This difficulty prompted Norris et al. (1983) to devise a technique in which individual $Ly\alpha$ lines are shifted to their rest frame wavelengths and all rest frame spectra are co-added. The most prominent metal element transitions can then be searched for in this high signal-to-noise averaged spectrum, yielding abundance measurements or upper limits. Along this approach, Lu (1991) estimated that the relative abundance of carbon of the LCs is roughly $[C/H] \sim -3.2$, where [C/H] represents the default

value and equals to $log(C/H) - log(C/H)_{\odot}$, from photoionization models. However, using a larger sample than Lu's, Tytler & Fan (1994) found only an upper limit of $10^{-2}$; More recently, Savaglio & Webb (1995) re-examined the chemical composition of the LCs using similar technique and showed that the derived abundance depends on the various observational quantities. Clearly, this kind of technique is limited by knowing the UV flux impinging on the clouds to a reasonable accuracy, since ionization correction plays an important role in determining the metal abundance of the LCs. Thus the lack of information in the spectral shape, intensity, and evolution with redshift of UV background produce an uncertainty on determining metal abundance.

Very recently, Tytler (1995) reported that CIV lines are measured in 60% of the high redshfit LCs with $logN(HI) \geq 14.5$. This implies that 50% of the LCs have metallicity $[C/H] \geq -2.5$. Using very high S/N, high spectral resolution data obtained with the HIRES spectrograph on keck 10 m telescope, Cowie et al. (1995) found that roughly half of the LCs with $N_{HI} \geq 3 \times 10^{14}\, cm^{-2}$ have measurale CIV lines with $N_{CIV} \geq 10^{12}\, cm^{-2}$. The ratio of the median column density of CIV to the median $N_{HI}$ to be $2 \times 10^{-3}$, roughly corresponding to a metallicity of $10^{-2}$ solar. This seems to be comparable to that of LLSs.

All these recent detections seem to imply a evidence that the most of the LCs contain metal elements. The previous thought that LCs are primordial is no longer tenable. If all LCs have metal, most probably metal in the LCs could have three origins: gas ejected from galaxies, pre-galactic massive stars and very massive objects, or star inside individual intergalactic LCs.

However, it could still be true that at high redshfit $z \geq 3$ the LCs have primordial composition. Accepted this hypothesis, by studying the ratio of deuterium to hydrogen in the high redshfit LCs, one can constrain the standard Big Bang nucleosythesis (SBBN) (e.g. Peebles, 1966; Walker et al. 1991). The advantage of this approach is less suffered from evolution effect. Two groups (Songaila et al. 1994; Carswell et al. 1994) independently found that the ratio $D/H \sim 2.5 \times 10^{-4}$, $\sim 10$ times the value of $D/H$ observed in the interstellar medium, from the redshfit $z = 3.32$ LLS in the spectrum of QSO 0014+813 ($z = 3.42$). According to SBBN, such a high ratio of $D/H$ requires a very low baryon content, $\Omega_b h^2 \sim 2.9 \pm 0.6 \times 10^{-3}$, in the Universe.

## 4.8 Proximity Effect

The number of the LCs per unit redshift increases with redshfit and empirically has a power law form as follows:

$$\frac{d\aleph}{dz} \propto (1+z)^{\gamma}. \tag{4.8}$$

A lot of efforts have been contributed to determine the value of index $\gamma$ (e.g. MHPB 1986; Tytler 1987). However, a confusing range of estimates of $\gamma$ has been produced by different authors. As pointed out by MHPB, this confusion has been caused, in part, by the "Proximity effect" in the cloud distribution: a decline in the number of the LCs arises as one approaches the QSO. This effect is discovered by Carswell et al. (1982) and studied by Murdoch et al. (1986), Tytler (1987),Bajtlik et al. (BDO, 1988), Lu et al. (1991), and Bechtold et al. (1993). The standard interpretation of this effect is that the extra ionizing radiation from the QSO reduces the neutral fraction in nearby clouds and it results in a defect in the number of clouds near a QSO in a neutral hydrogen column density limited sample compared to that expected in an ensemble of all QSOs.

On the basis of photoionization models, if the clouds are highly ionized and optically thin, the neutral hydrogen column density $N$ of a cloud near a QSO is

$$N = \frac{N_0}{1+\omega}, \tag{4.9}$$

where $N_0$ is what the column density would have been if there had been no nearby QSO, and $\omega(z, z_Q) = J_Q/J_B$ is the ratio of the Lyman limit QSO intensity impinging on an cloud to the background intensity at the same frequency (BDO).

Strictly speaking, Eq.(4.9) is valid only if the frequency dependence of the background radiation above the Lyman limit is same as that of the QSO radiation, so that the ratio of ionization rates equals to the ratio of Lyman limit intensities. The distribution of observed cloud number in column density has been shown to be approximated by

$$\frac{d\aleph}{dN} = BN^{-\beta}. \tag{4.10}$$

Then the number of clouds above a given threshold $N_{min}$ is

$$\aleph(N \geq N_{min}, \omega = 0) = \frac{BN^{-(\beta-1)}}{\beta - 1}. \tag{4.11}$$

On the other hand, the number of clouds above a given threshold $N_{min}$ near the QSO is

$$\aleph(N \geq N_{min}, \omega) = \frac{BN^{-(\beta-1)}}{\beta - 1}(1+\omega)^{-(\beta-1)}. \tag{4.12}$$

For $N_{HI}$ limited sample,

$$\frac{N(\omega)}{N(\omega = 0)} = (1+\omega)^{-(\beta-1)}. \tag{4.13}$$

Hence for a sample limited by the observed neutral hydrogen column density $N_{min}$, the distribution of clouds with redshift, including the QSO proximity effect, is

$$\frac{d\aleph}{dz} = A(1+z)^{\gamma}(1+\omega(z))^{-(\beta-1)} \tag{4.14}$$

with

$$\omega(z) = \frac{f_Q}{4\pi J_B(z)} \frac{(1+z)^5}{(1+z_Q)} [\frac{(1+z_Q)^{0.5} - 1}{(1+z_Q)^{0.5} - (1+z)^{0.5}}]^2 \quad \Omega_0 = 1. \tag{4.15}$$

The proximity effect should be stronger as QSO luminosity increases (BDO). But, Lu et al.(1991) found no positive evidence that the proximity effect is correlated significantly with the QSO luminosity, contrary to previous results. More recently Bechtold(1994) indeed found that the strength of the proximity effect depends weakly on QSO Lyman limit luminosity. This supports the standard interpretation that proximity effect results from enhanced photoionization by the QSO's UV radiation, rather than some property of the QSO or the IGM which evolves with redshift.

According to this standard interpretation, it would mean that at the distance from the QSO where the density of lines is half the universal value, observed flux of ionizing radiation from the QSO is comparable to the mean ionizing background. This provides a way to determine the intensity of ionizing background. The inferred value of intensity of metagalactic UV field at Lyman limit is $J_{21} \approx 1$ (BDO). However, the value derived by Bechtold

(1994) is about a factor of 3 larger. Whereas, lower values have been derived from a reanalysis of the proximity effect (Espey 1993; Loeb & Eisenstein 1995).

From a tentative detection of the proximity effect at low redshift, $z \leq 1$. Kulkarni & Fall (1993) have estimated that at $z \sim 0.5$ the mean ionizing intensity at the Lyman edge is $J_{21}(z = 0.5) \sim 6 \times 10^{-3}$.

## 4.9 Fundamental Equations for Structure and Evolution of the LCs

Despite the recent observational advances, progress in theoretical understanding of the origin, structure and evolution of the LCs has not been as rapid. There is no definitive model, although a multitude of possibilities has been suggested. For instance, regards as the physical origin of the LCs, there are three reasonable scenarios that produce the observed LCs. In a simple, hierarchical structure formation model there was first an IGM, it clumped together small scales to form the LCs, and these gradually merged together to make larger structures. Alternatively, the IGM could still be primarily leftover from galaxy formation, but Jean's mass constraints could lead to galaxy formation, followed by later fragmentation to form the LCs, or ejection of them as proposed by Wang (1995). Finally, perhaps galaxies formed first and efficiently, and produced a considerable, moderately hot IGM by hydrodynamic feedback. This IGM may have been necessary to confine the LCs so that they were the last structures to form. Unfortunately, the physical origin of the LCs has still remained a mystery so far (Cen et al. 1994).

Despite the uncertainties on the origin of the LC, the fundamental equations for studying the structure and evolution of the LC are unambiguous. They are the continuity equation, the equation of motion, the equation of energy conservation describing the evolution of temperature, and the chemical evolution equation. Under given initial condition and boundary condition, one can numerically solve the set of the differential equations and obtain the detailed information about structure and evolution of clouds. Comparison with observations, one can check the availability of the models.

1. **Equation of Continuity**

$$\frac{\partial \rho}{\partial t} + \nabla \cdot (\mathbf{u}\rho) = 0, \tag{4.16}$$

where $\rho$ is mass density, $\mathbf{u}$ is velocity of fluid element.

2. **Equation of Motion**

$$\frac{\partial \mathbf{u}}{\partial t} + \mathbf{u} \cdot \nabla \mathbf{u} + \frac{1}{\rho} \nabla p = -\nabla \phi, \tag{4.17}$$

where p is a gas pressure, $\phi$ is gravitational potential.

3. **Equation of Energy Conservation**

$$\frac{\partial T}{T \partial t} = (\gamma - 1)[\frac{(\Gamma - \Lambda)}{y_t n_H k_B T} + \frac{\partial n_{II}}{n_H \partial t} + \frac{\partial y_t}{y_t \partial t} - \frac{\partial}{\partial t}(\frac{1}{\gamma - 1})] + \frac{\gamma}{\mu} \frac{\partial \mu}{\partial t}, \tag{4.18}$$

where $\Gamma$ is heating the rate, $\Lambda$ is the total cooling rate excluding expansion, $y_t = \Sigma y_i$, with $y_i = \frac{n_i}{n_H}$ being the concentration of the ith species, and the mean molecular weight is given by $\mu = \frac{\Sigma y_i \mu_i}{y_i}$. The mass density of the cloud is $\rho = n_H \Sigma y_i \mu_i$.. The above form of the energy conservation is derived from the first law of thermodynamics.

4. **Equation of Chemical Evolution for Hydrogen**

$$\frac{\partial y_{HI}}{\partial t} = n_e(1 - y_{HI})\alpha_H(T) - n_e y_{HI} c_H(T) - 4\pi y_{HI} \int_{\nu_{HI}}^{\infty} \frac{J_\nu}{h\nu} \sigma_{HI} d\nu \tag{4.19}$$

where the first term of the right side of the equation represents the rate of recombination to neutral hydrogen, the second gives the ionization rate due to collision and the third does the photoionization rate. We present only one equation for Hydrogen here. Actually, there is one chemical evolution equation for each species.

Above equations combined with the radiation transfer equation form a complete set of equations. Given initial condition and boundary condition, the structure and evolution of clouds can, in principle, be known. In fact, above

differential equation set is very complicated, so some approximations for simplicity are necessary in calculations.

The approximation used by different authors depends on their aim. In 1980s, the thermal equilibrium instead of the equation of energy conservation was usually adopted. This kind of approximation made a big simplicity, but recently it was found that it seems to be not accurate enough. Meiksin(1994) performed detailed numerical simulation in the context of the mini-halo model. These calculations do not assume the clouds to be in hydrostatic or in thermal equilibrium. He consider also the fact that matter is constantly accreting from outside the cloud. One of the distinct features of his results is that a cloud may be identified into three zones: a quasi-hydrostatic core in thermal equilibrium; a nonhydrostatic intermediate zone out of thermal equilibrium; and a cosmological accretion layer joining onto the Hubble expansion. This character should not be unique for his model, but come from the assumed initial perturbation profile. An different initial perturbation profile may result in an different structure of the LC.

The picture of the LC is still being adjusted by knowledge of new data. The observed number density distribution function of LCs with redshift and neutral hydrogen column density still allows many possible theoretical models.

## 4.10 Confinement Mechanisms

The essential observational fact, that has to be interpreted by any theoretical model, is that the LCs have a several tens kiloparsec sizes and are typically separated by $\sim 2Mpc$ along the line of sight, but produce most of the absorption. This requires that the absorption per unit length within a LC must exceed the absorption per unit length in the diffuse IGM by a factor of more than $10^2$ (this value depends on the size of the LCs). Because the neutral hydrogen number density is proportional to the square of total hydrogen number density, the clouds must then be overdense by a factor $> 10$. This has led to extensive discussions of possible confinement mechanism, with gravity and external gas pressure being proposed, as well as free expansion.

### 4.10.1 Gravity Confinement

Given the assumption of photoionization equilibrium, the ratio of the gravitational energy to the thermal energy of a spherical clouds is (Ostriker 1988)

$$\mid \frac{W}{U} \mid = \frac{GM_c m_H}{5ktR_c} = 9 \times 10^{-4}(1+z)^{1/4}(N_{14}J_{21})^{1/2}(R_c/11kpc)^{3/2}. \quad (4.20)$$

Therefore, under a typical condition, $\mid W/U \mid \sim 10^{-3}$. So the self-gravity by baryonic matter in the clouds can not confine gas. Rees(1986) and other authors (Ikeuchi 1986; Ikeuchi et al. 1988) proposed a minihalo model. In this model the LCs were taken to be spheres in hydrostatic equilibrium, confined by the gravity of a cold dark matter "mini-halo". The confining halos were envisioned to have smaller masses than ordinary galaxy halos, with velocity dispersions of the order of tens of $km/s$. This model has considerable predictive power as demonstrated in some recent papers (Miralda & Rees 1993; Mo et al. 1993; Meiksin 1994). Their calculations show that the density falls off rapidly with radius, so this model has a virtue to produce a large range of neutral hydrogen column density from a single cloud. The shortcoming of mini-halo model is difficult to interpret the observed large cloud sizes (Bechtold et al. 1994; Dinshaw et al. 1994). There is another version of minihalo model which confine gas in a slab geometry. However, it also meets problem of the large cloud dimensions.

### 4.10.2 Pressure Confinement

This model was first discussed in the classic paper by SYBT (1980). The critical point that remains clouds overdensity in this model is that the external gas pressure roughly balance against the cloud diffuse. Since the density of external gas is far smaller than one of the cloud, to confine it, the temperature of the external gas has to be much higher than one of the cloud. Ostriker and Ikeuchi(1983, 1986) pointed out that the shock may heat the temperature of the external gas to such a high temperature. The product of the density and the temperature of the cloud must balance with the external pressure. The pressure could be local to the clouds (in surrounding hot halos), or at the opposite extremely it could be a uniform IGM. This model has been developed by Ikeuchi & Ostriker (1986) and by Baron et al.(1989). It is easy to interpret the large cloud dimensions in this model, but it has been

found to have a serious problem (Williger & Babul 1992). Assumed ionization equilibrium, the large range of neutral hydrogen column density for the LC population ($10^{13}-10^{17}\ cm^{-2}$) requires a range of twelve orders of cloud masses (Charlton 1995). It is too large magnitude to be realistical. Furthermore, confining clouds with neutral hydrogen column density larger than $10^{16}\ cm^{-2}$ would require a high temperature of external gas that are likely to exceed constrains placed by the COBE y-parameter limits (Mather et al. 1994). As a consequence of existing a high temperature intergalactic gas, the thermal velocity of electrons should perturb the angular distribution and spectrum of cosmic microwave background radiation through Compton-Thomson scattering. The recent spectrum measurements by the COBE satellite indicate that the spectrum distortion is quite small and place a strong constrain on the temperature of IGM.

Barcons and Fabian (1987) considered also a model of pressure confined slabs. However, this model suffers similar problem to that spherical model does.

### 4.10.3 Mixed Gravity and Pressure Confinement

It is possible, and in fact natural, that more than one mechanism are responsible for cloud confinement. Several authors (Salpeter 1993, 1994; Hoffiman et al. 1993; Salpeter & Hoffiman 1995) proposed that a cloud has two distinct regions: its inner region (with higher $N_{HI}$) gravity confined and its outer region (with smaller $N_{HI}$) pressure confined. In this class of model the column density is exponential near the center, but switches to a power law form, which may continue out to radii of a couple of hundred $kpc$. In this way it is possible to have very large cloud sized without an unreasonable range of mass. The boundary between the inner, gravity confined and the outer, pressure confined is depended on the the value of the external pressure. Considering both exists of the external pressure and the gravity, the equation of hydrostatic equilibrium can be written as (Charlton et al. 1993, 1994)

$$\frac{\pi}{2} G m_H^2 \eta N_{tot}^2 + P_{ext} = P_{cloud}. \tag{4.21}$$

where $\eta$ is the contribution to gravity due to dark matter relative to that of ordinary gas, $N_{tot}$ is total hydrogen column density, and $P_{ext}$ and $P_{cloud}$ are the temperatures of external gas and cloud respectively. The gravitational

and pressure forces are equally important at specific value of

$$N_{ext} = N_1(\frac{2}{\pi}\frac{P_{ext}}{Gm_H^2\eta})^{1/2}. \tag{4.22}$$

For $N_{ext} < N_1$ the cloud is pressure confined and $N_{HI} \propto N_{tot}$. In the gravity confined regime (for $N_{ext} > N_1$), we roughly have $N_{HI} \propto N_{tot}^3$.

The different relationships between $N_{HI}$ and $N_{tot}$ translate to a prediction for the distribution function with HI column density for clouds. For a suitable given distribution function with total hydrogen column density, one get $\beta = 1.8$ in the pressure dominated regime and $\beta = 1.3$ in the gravity dominated regime. This type of shape for $f(N_H)$ is fit to the data of Petitjean et al. (1993a). However, this feature (the flattening in column density distribution at $N(HI) \sim 10^{16}\, cm^{-2}$) can alternatively explained in terms of a transition between metal-poor and metal-rich systems (Petitjean et al. 1993a).

# Chapter 5

# Metal Absorption Systems (MASs)

The absorbers identified by metal absorption lines are called metal absorption systems (MASs) (Weymann et al. 1979; Young, Sargent, & Boksenberg 1982). This population have been extensively studied since the late 1980s. In general the strongest metal absorption lines are the CIV and MgII doublets. A MAS with detected CIV absorption line is usually called a CIV system and one with detected MgII absorption line called a MgII system.

At high redshifts ($z \geq 2$), the population of metal absorbers comprises two subclasses which are characterized by the presence or absence of low-ionization species (CII, MgII, FeII). Assuming that these absorbers are photoionized by the UV metagalactic field, it has beeen shown that the difference between these two subclasses of absorbers (CIV only or mixed systems) mainly arises from an opacity effect. The phase which contains singly ionized ions has a large optical depth at the Lyman limit. On the other hand, at low redshift, the low-ionization systems do not always trace high opacities, as is the case at high redshfit (Bergeron et al. 1994).

In the $z \sim 1.3-2$ sample of Lanzetta (1987), the fraction of CIV systems with associated MgII absorption is roughly one-half. From a larger MgII absorption survey down to an equivalent width limit $w_{lim}(MgII\lambda = 2796) = 0.3\AA$, Steidel & Sargent (1992) have found that, in the redshift range $1.2-2.2$, 73% of the system have only CIV absorption and that there is just one case (1%) with MgII detected but not CIV.

Frequently, the CIV systems show complex structure, consisting of many

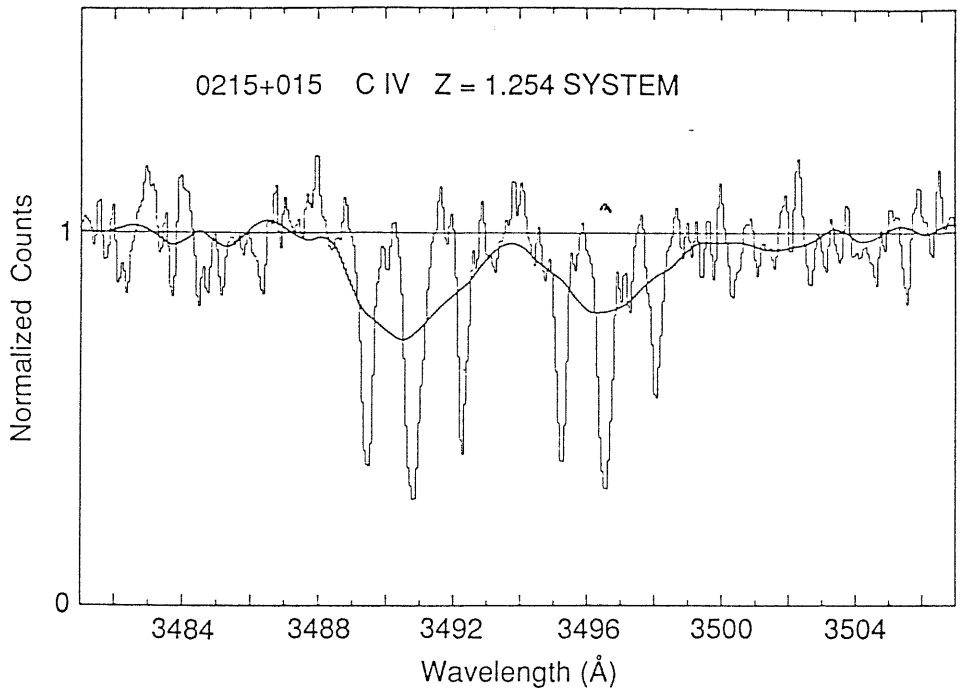


Figure 5.1: A comparison of the same CIV doublet in Q0215+015 obtained at Two different resolutions, first shown by Pettini (1995). The lower resolution spectrum (from Blades et al. 1982) is at 120 $kms^{-1}$ FWHM and only reveals the presence of a single CIV doublet. The higher resolution spectrum reveal more precisely the nature of the absorption. Taken from Blades (1988).

components spread over large velocity range, typically from 100 to 1000 $kms^{-1}$. Figure 5.1 compares two observations taken at widely different resolutions of the same CIV doublet. The apparently single CIV doublet at low resolution is shown to consist of at least three separate components for which accurate column densities and Dopper width can be determined. This multi-component structures shown at high resolution make difficult to derive column densities from measured equivalent width at low resolution based on the curve of growth analysis.

The MASs are widely believed to originate in galactic halos. The main reason for this belief are as follows: (1) They contain some amount of metal

elements. (2) The two-point correlation function for the CIV systems shows a positive clustering feature in $\Delta v \leq 300\, kms^{-1}$, which is the same as that of galaxies (Sargent et al. 1988). (3) More than ten MgII systems have been identified with galaxies ($0.16 \geq z \leq 0.79$) on the lines-of-sight to QSOs (Bergeron 1988). (4) The average size is estimated to be several tens of kiloparsecs from the observed rate of incidence of the absorption systems in the QSO spectra. Thus, the MASs may be used to study directly the evolution of galaxies (including both structure and chemical evolutions) at redshifts inaccessible to any other means of observation.

Generally speaking, the most of MASs, if not all, have large HI column densities. Ones of them which have a column density larger than $1.6 \times 10^{17}\, cm^{-2}$, corresponding to the optical depth at HI limit edge larger than unit, are specially called Lyman limit systems (LLSs). Unlike the LCs, which remove light over a very restricted range of wavelengths in a spectrum, the LLSs produce strong continuum absorption at all wavelengths $\lambda_{obs} \leq (1 + z_{obs})912\text{Å}$. They include most MgII systems, many CIV systems, and about 20% of them are Ly$\alpha$-only systems (e.g. Sargent et al. 1988). They are important for several reasons. First, the LLSs represent the parent population from which absorbers that are selected on the basis of the MgII $\lambda\lambda 2796, 2303$ resonance-line doublet are drawn (Lanzetta, Turnshek, & Wolfe 1987). The MgII-selected systems –or at least those systems at redshifts $z \sim 0.5$–have recently been shown to originate in the extended halo regions of bright galaxies (Bergeron 1988; Bergeron & Boissè 1990), which suggests that most or all of the LLSs are also associated with galaxies. So, the study of the LLSs will provide some information on the formation of galaxies. Second, because the LLSs are detected on the basis of continuous rather than line absorption, the systems are selected without regard to the kinematic or multiple-component structure (Lanzetta 1988). As a consequence, a sample of LLSs represents a complete sample of optical thick absorbers, whereas a sample selected on the basis of the MgII or CIV doublet is biased toward detecting systems with velocity components and large velocity spreads (Blades 1988). Finally, because the unique spectroscopic signature of the LLSs may be easily recognized even in data of relatively low quality, the absorbers can be detected at low redshifts with IUE spectra as well as higher redshifts with optical spectra. It is therefore possible to study the evolution of the properties of the systems over a larger fraction of the present age of the Universe.

## 5.1 Photoionization Model

Because of the limitation of observations, in order to obtain more information than that directly derived from observations, an ionization theory is needed. The possible ionization mechanisms have photoionization, collisional ionization, or ionization by shock. The first is most likely one favored by several observations. The fundamental equations of photoionization model are the equations of photoionization equilibrium and thermal equilibrium. Assuming that all ions are in their ground level and the ionization field is not very intenser, the photonization rate of an ion $X(i)$ with a number density $n^{X(i)}$ is

$$4\pi n^{X(i)} \int_{\nu_i}^{\infty} \frac{J_\nu}{h\nu} \sigma_\nu X(i) d\nu = n_\epsilon n^{X(i+1)} \alpha_A(X(i), T), \tag{5.1}$$

where $J_\nu$ is the mean intensity of radiation; $\sigma_\nu X(i)$ is the photoionization cross section from the ground level of $X(i)$ with the threshold $\nu_i$; $n_\epsilon$ is the electron density and $\alpha_A(X(i), T)$ is the recombination coefficient of the ground level of $X(i+1)$ to all levels of $X(i)$.

The equilibrium temperature of the gas is the result of the balance between heating, by absorption of the UV photons, and cooling via several atomic processes. The most important cooling processes have been summarized in the chapter 3. One may write the equation of thermal equilibrium as follows:

$$\Gamma = \Lambda, \tag{5.2}$$

where $\Gamma$ it the heating rate and $\Lambda$ is the cooling rate.

The conservation equation of total number of ions of all stages of ionization is

$$n^{X(1)} + n^{X(2)} + \cdot + n^{X(m)} = n^X. \tag{5.3}$$

If ignoring the change of ionizing radiation inside a absorber by absorption and re-emission by the absorber, the above equation set completely determines the fractions of all ionization species. In principle one can use the equation of radiative transfer to deal the influence on ionizing field by matter. However, it will introduces a big complication into calculation.

Evidently, the degree of ionization depends on the ratio of the ionizing photon flux to the gas density. This ratio is traditionally called the ionization

parameter. The ionization parameter for hydrogen, on the surface of the absorber, is given by

$$U = 4\pi \frac{\int_{\nu_{HI}}^{\infty} J_\nu / h\nu d\nu}{cn_e}, \tag{5.4}$$

where c is the speed of light which is introduced to make $U$ dimensionless.

Actually there is a different ionization parameter for each ion and at each point in the absorber. However, in practice, $U$ as defined for hydrogen on the surface of the absorber, is very useful and characterizes the overall of ionization very well. But, if the spectrum of ionizing field deviates far away from a pawer law (e.g. existing a big break at HeII edge in the spectrum). only one ionization parameter for hydrogen is not adequate to characterize the overall level of ionization.

By comparison the observed column density ratios with those predicted by photoionization models, one may locate the allowed range of $U$ which gives the appropriate column density ratios. Carbon is the best element to use in constraining $U$ for CIV systems for several reasons: first, for whole range of $U$ being considered, at least 90% of the C is expected to be in the form of CII, CIII, and CIV, and lines of all three ions are observable. The ratio $N(CIV)/N(CII)$ is particularly sensitive discriminant since it change rapidly with $U$ (see Fig 11, Steidel 1990a), and lines of both ions are observable longward of the Ly$\alpha$ emission line (and therefore free of the confusion present in Ly$\alpha$ forest).

In the case in which the spectrum of radiation flux is a power law $J(\nu) \propto \nu^{-\alpha}$, the range of $U$ found for CIV system is two decades around $U \sim 10^{-3}$. This is ture for $1 \leq \alpha \leq 2$, but this range is slowly shifted toward higher value of $U$ when $\alpha$ increases (Steidel 1992; Bergeron & Stasinska 1986). For MgII system, a ratio $N(MGII)/N(FeII) \sim 1$ requires very low value of $U$ at most $U \sim 10^{-4}$.

## 5.2 Evolution of Number Density with Redshift

For Friedmann models with zero cosmological constant and a deceleration parameter $q_0$, the number of absorption line systems per unit redshift is

given by

$$\frac{d\aleph}{dz} = n(z)\sigma(z)\frac{c}{H_0}(1+z)(1+2q_0z)^{-0.5} \tag{5.5}$$

where $n(z)$ and $\sigma(z)$ are the co-moving density and projected cross-section on the sky of the absorbers at redshift $z$, c is the speed of light, $H_0$ the Hubble constant. This function of $z$ is usually approximated by a power law

$$\frac{d\aleph}{dz} \propto (1+z)^{\gamma} \tag{5.6}$$

For a non-evolving cloud population, $\sigma\rho_0$ is constant and $d\aleph/dz$ then depends weakly on redshift. $\gamma = 1$ for $q_0 = 0$ and $\gamma = 1/2$ for $q_0 = 1$. $\gamma$ significantly greater than 1 indicates the strong evolution in the number density of absorbers. The statistical analysis of the MASs and the LLSs is difficult and uncertain due to the small size of the samples. Despite of this fact, a lot of efforts have been contribute to determining the value of evolution parameter $\gamma$. The main results are summarized in table 4.1. From above table, it is apparent that the comoving density of CIV systems is decreasing with increasing redshift. This evolving behaviours of CIV is different from those of MgII systems and the LLSs. The natural interpretation of this result is that at redshift $z \geq 2$ the LLSs evolves into CIV-selected systems with time (Lanzetta 1991). This suggests that the observed evolution of the CIV absorbers is not due to chemical enrichment of the absorbing gas but in fact indicates a systematic evolution of the ionization level of the absorbers. On the basis of photoionization model, the observed evolution may be explained if the ionization parameter $U$ increases with decreasing redshift by a factor of roughly 3 within the redshift interval $2.5 < z < 3.7$. This change in $U$ could be due to the evolution of ionization background or the local ionizing source. Alternatively, it might arise as a result of evolution of the average gas density of the absorbers.

Very recently, Boksenberg (1995) investigated that the evolution of LLSs over a wide redshift range using HST observations (26 QSOs) combined with high quality data selected from previously available optical and IUE observations and new optical observations. They found that the total data (169 QSOs) were well fitted by a single power law with $\gamma = 1.50 \pm 0.39$.Lombardi (1995) also found a closed value of $\gamma$ 1.55. If this slow evolution of the LLSs is confirmed, the idea of the LLSs evolving into the CIV systems is no longer correct.

Table 4.1. Estimates of $\gamma$
(compiled from the literature)

| | | system | z | $\gamma$ |
|---|---|---|---|---|
| Tytler | 1982 | LLSs | | $1.7\pm$ |
| Bechtold et al. | 1984 | 21LLSs | 1-3.5 | $1.3 \pm 1.5$ |
| Lanzetta et al. | 1988 | 53LLSs | 0.36-3.78 | $0.48 \pm 0.45$ |
| Sargent et al. | 1989 | 54LLSs | 0.67-3.58 | $0.68 \pm 0.54$ |
| Lanzetta | 1991 | 92LLSs | 0.35-2.5 | $0.3 \pm 0.9$ |
| | | | 2.5-3.7 | $5.7 \pm 1.9$ |
| Lanzetta et al. | 1987 | 22MgII | 0.9-2.1 | $2.4 \pm 0.8$ |
| Boksenberg | 1995 | 169LLSs | $< 4.$ | $1.50 \pm 0.39$ |
| Lombardi et al. | 1995 | LLSs | $< 4.$ | $\sim 1.55$ |
| Sargent et al. | 1989 | 66MgII | 0.15-2.15 | $1.45 \pm 0.63$ |
| Steidel & Sargent | 1992 | 111MgII | 0.2-2.2 | $0.78 \pm 0.42$ |
| Aldcroft et al. | 1994 | 80 MgII | $\sim 1.13$ | $1.11 \pm 0.46$ |
| Bergeron & Boissé | 1984 | 47CIV | 1.4-2.0 | $1.8 \pm 2.0$ |
| Sargent et al. | 1988 | 229CIV | 1.2-3.53 | $-1.2 \pm 0.7$ |
| Steidel | 1990 | 275CIV | 1.3-4.0 | $-1.26 \pm 0.56$ |

## 5.3 HI Column Density Distribution of the LLSs

The distribution of HI column densities of the LLSs has been investigated by Tylter (1987), Bechtold (1987), Sargent et al. (1989) and Lanzettea (1991). HI column densities of the optically thick absorbers may accurately determined only for $17.2 \leq log[N(HI)/cm^{-2}] \leq 17.7$ based on measurable optical depths at the Lyman limit and for $log[N(HI)/cm^{-2}] \geq 20.3$ based on profile fits to damped Ly$\alpha$ absorption lines. For intermediate column densities i.e. for for $17.7 \leq log[N(HI)/cm^{-2}] \leq 20.3$, it is possible only to derive limits on the HI column densities based on the absence of residual flux at wavelengths shortward of $\lambda_{912}$ and on the absence of strong damped Ly$\alpha$ absorption lines.

The column density distribution function is usually assumed to have a pawer law form

$$\frac{d\aleph}{dN_{HI}} = BN(HI)^{-\beta}. \tag{5.7}$$

The value of $\beta$ found by Bechtold (1987) is $0.8 \pm 0.2$; the value of $\beta$ found by Sargent et al. (1989) is 1.39. More recently, Lanzetta (1991) used a bigger sample to obtain $\beta = 1.25 \pm 0.03$. The value of $\beta$ found by Lanzetta is consistent with that found by Sargent et al. (1988), but is inconsistent at the $4.3\sigma$ level with that found by Bechtold (1987). The reason for the discrepancy may be the very large uncertainties in the intermediate column densities range.

By comparison with the column density distribution function of the LCs, if accepted the value of $\gamma \sim 1.5$ for the LLSs, there is no change in slope around $log[N(HI)/cm^{-2}] \sim 17$, at which point an HI cloud would become optical thick. Furthermore, the observed density of the LLSs is consistent with the value predicted by extrapolating the power law fit to the LCs alone up to the column densities of the LLS. Partly based on above facts, Tytler (1987) suggested that both the LCs and the LLSs belong to the same population and have same origins and the same spatial location.

Although the LC and the LLS column density distributions join together smoothly around $log[N(HI)/cm^{-2}] \sim 17$, there are a lot of authors (e.g. Sargent et al. 1989) who do not agree with Tytler that there is, in reality, one population of absorbers. Because the LCs and the LLSs differ considerably both in their evolution in redshift and in their clustering properties.

## 5.4 Equivalent Width Distribution of MgII or CIV Absorption Lines

The distribution functions of rest equivalent widths of both MgII absorption lines (for MgII systems) and CIV absorption lines (for CIV systems) have been examined by many authors (SYBT 1980; Tytler et al. 1987; Lanzette et al. 1987; Sargent et al. 1988; Steidel 1990a, b; Steidel & Sargent 1992). Usually the functional form of equivalent width distribution is assumed to have an exponential form found by SYBT (1980) for the LCs, namely

$$\frac{d\aleph}{dW} = (\frac{\aleph^*}{W^*})e^{-\frac{W}{W^*}}, \tag{5.8}$$

where $\aleph^*$ and $W^*$ are parameters to be determined.

However, in fact, above exponential distribution is probably not appropriate for either of MgII data or CIV data, as mentioned by Steidel (1990a).

In any case, one can expect in principle to derive a MgII or CIV column density distribution function from the equivalent width distribution using the curve of growth analysis. For determining the MgII or CIV column density distribution, the main difficulty arises from the fact that the most CIV systems and considerable MgII systems have complex velocity structure, consisting of many components spread over large velocity ranges, typically from $10^2$ to $10^3\, kms^{-1}$. Moreover, large variations in the strengths of components occur from species to species. This picture has now been rather firmly established by high-resolution observations (e.g. Blades 1988; York et al. 1984; Pettini et al. 1983; Petitjean & Bergeron 1990, 1994). Thus, for spectra with moderate-resolution, the components will be unresolved and the measured equivalent widths of the lines represent the ensemble equivalent widths. However, Jenkins (1986) has shown through simulation involving ensemble of clouds having a distribution of column densities and b values that the total column densities inferred on the basis of moderate-resolution spectra agree remarkly well with those determined on the basis of spectra in which the individual velocity components are resolved. The most important result found by Jenkins (1986) is that a single-component curve-of-growth analysis can be used to infer total column densities for each system. Unfortunately, up to now, neither MgII or CIV column density distribution has been presented.

Table 5.2. Estimate of $W^*$

| | | system | z | $\aleph^*$ | $W^*\AA$ |
|---|---|---|---|---|---|
| Lanzetta et al. | 1987 | 22MgII | 0.9-2.1 | $1.76 \pm 0.40$ | $0.88 \pm 0.19$ |
| Steidel & Sargent | 1992 | 111MgII | 0.2-2.2 | $1.55 \pm 0.20$ | $0.66 \pm 0.11$ |
| Sargent et al. | 1988 | 229CIV | 1.2-3.53 | $5.92 \pm 0.59$ | $0.4 \pm 0.02$ |

## 5.5 Spatial Distribution and Correlation with the QSOs

Bahcall and Peebles (1969) first proposed a statistical test to examine the distribution of number of absorbers observed per QSO. If absorbers are cosmologically distributed, the distribution of the number of independent absorbers per QSO is a Poisson distribution. In early 80s, Young et al. (1982) performed this kind of test and found that their result is consistent with that expected by Bahcall and Peebles (1969).

Following the work of Peebles and co-workers on the distribution of galaxies, the two-point correlation function has become the commonest description of the clustering of absorbers in velocity down the individual lines of sight to QSOs. For each QSO, one forms all possible pairings of absorbers. The separation of each pair is calculated in either velocity, or comoving distance $r$. The two-point correlation function is estimated from $N_{obs}(r)$, the observed number of separations in $(r, r+dr)$, and $N_{exp}(r)$, the expected number from the Poisson distribution.

$$\xi(r) = \frac{N_{obs}(r)}{N_{exp}(r)} - 1. \tag{5.9}$$

It has been found that CIV systems cluster strongly on scales of under $1000\,kms^{-1}$ (Sargent et al. 1988), and in a few QSOs out to $10000\,kms^{-1}$ (Heisler et al. 1989). MgII systems also cluster on scales of under $600\,kms^{-1}$ (Petitjean & Bergeron 1990). It is suspected that the CIV and MgII systems cluster like galaxies, but this is hard to prove (Heisler et al. 1989).

The large scale structure of the Universe can be studied at high redshfit using the MASs, which have been shown to represent the halos of luminous

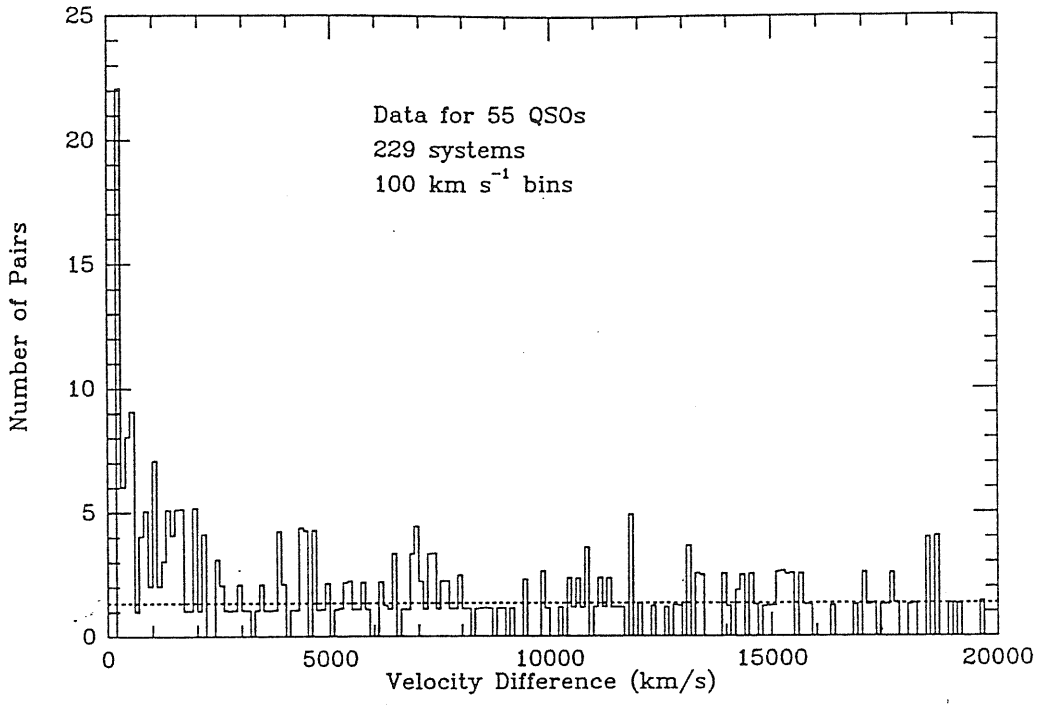


Figure 5.2: The two-point correlation function for CIV absorption systems. The dotted line represents the adopted background level or the mean number of pairs per bin $< N_p >$. The correlation amplitude for each bin is then $\xi = (N_{obs}/ < N_{exp} >) - 1$. Taken from Sargent et al. (1988).

galaxies. Impey & Dinshaw (1995) calculated a spatial correlation function using a total of 47 CIV absorbers distributed among the four lines of sight, and found the dimensions of the hypothetical supercluster at $z = 2$ to be at least $40 Mpc$ on the plane of the sky and about 60 Mpc along the line of sight. The clustering amplitude on these scales is larger than is predicted by current theories of the formation of large scale structure.

A cross correlation of strong CIV absorbers with QSOs has also been found in a highly significant level (99.84% confidence) (Møller 1995). The strength of the QSO/absorber correlation inside those $10h^{-1}Mpc$ structure is $\sim 3.4^{+1.5}_{-1.1}$. The correlation peak is found at an ejection velocity of about $1500\, kms^{-1}$ with respect to the QSOs. It is ruled out at the 99% confidence level that the weak CIV doublets, $W_{rest} < 0.3\mathring{A}$, are clustered the same way as the strong lines. The implication of this different clustering behaviours is that the two classes of absorbers are truly different, and that it is likely that they do not occupy the same volumes of space. The weak absorbers could be either evenly distributed like the LC, or they could be the high velocity tail of the ejected systems as suggested by Weymann et al. (1979).

## 5.6 Metallicity of the MASs

On the basis of measured column densities of a few ionization stages of metal elements and HI column density (not all ionization species can be observed simultaneously because the absorption lines cover a big range from far-UV to optical band) and using photoionization model, one may derive the abundances of metal elements. Determination of the abundances requires an accurate estimate of $N(HI)$ and observation of a large number of ionization stages. In fact, there are a number of uncertainties involved in the determination of the metal element abundances:

1. Evolution of the $n(HI)/n(H)$ Ionic Ratio

   It is a function of the ionization level of the metal elements and the spectral shape of the ionizing background radiation. This ionic ratio is better determined when the low ionization ions are the dominant species. The best cases are the damped Ly$\alpha$ systems for which $n(HI)/n(H)$ is very close to unity.

2. HI Column Density of the Absorber

Only for the relatively rare case in which $1 \leq \tau_{LL} \leq 3$ that an accurate estimate of $N(HI)$ could made on the basis of the low-resolution spectra. In general, high-resolution spectra of the Ly$\alpha$ line alone are not sufficient to determine uniquely the HI column density and velocity parameter $b$ for a high column density absorber, and such measurements result in a rather large range of possible combinations of parameters. because absorption lines, in this case, locate in saturated part of the curve of growth.

3. Ionization States of Metal Elements

   Their estimates depend on the ionizing radiation field and the HI column density of the absorber. Due to a poor knowledge of both intensity and spectral shape of ionizing background radiation. their values have fairly large uncertainties.

4. Velocity Dispersion of Individual Components

   Observations at high resolution ($R > 10^4$) have show that the strong CIV systems almost always break up into many narrow components spread over large velocity ranges. The estimate of abundance could be seriously in error if the dominant species are formed in different component.

From a survey of ZnII and CrII absorptions in high-redshift damped systems. Pettini et al. (1994) have derived abundances typically of one-tenth the solar values and a range $-1.5 \leq [ZnII/HI] \leq 0.0$, where [Z/H] represents the default value and equals to $log(Z/H) - log(Z/H)_{\odot}$. For the LLSs, Steidel (1990b) found that at $z \sim 3$ the metal element abundances are within the broad range $-3.0 \leq [Z/H] \leq -1.5$, whereas Bergeron & Stasińska (1986) and Petitjean, Bergeron, & Puget (1992) have derived somewhat larger values covering the range $-2.0 \leq [Z/H] \leq -0.5$ at $z \sim 2.5$. From the HST QSO absorption line survey (Bahcall et al. 1993, 1994), Bergeron (1994) derive a high metal element abundances, $-0.5 \leq [Z/H] \leq -0.3$ at $z \sim 0.5$ for the LLSs. More recently, Lanzetta et al. (1995) found that $[Z/H] = -1.0 \pm 0.5$ at $z \sim 2.5$ from the IUE survey for damped Ly$\alpha$ systems and the LLSs.

Spectroscopic UV observations with the HST of the OSQ HS 1700+6416 ($z = 2.72$) (Reimers et al. 1992; Reimer & Vogel 1993; Vogel & Reimer 1995) offer for the first time the possibility to measure column densities of C, N

and O simultaneously in several ionization stages (OIII to OVI, CIII and CIV, NII to NV). On the assumption of photoionization model, they found abundances $[C/H] = -1.7, -2.3, -1.9$ for $z = 1.8465$, 2.1678 and 2.433, respectively. There is also strong evidence for an enhances oxygence abundance relative to carbon and similar for an enhanced $[N/C]$. This survey is spread over a large energy range, with some lying above the HeII ionization potential and some below. Therefore it is possible to derive allowed spectral shape. One of the striking features of their observations is that the observed neutral HeI column density is higher by a factor of $\sim 5$ than that predicted by a photoionization model with a typical spectral shape. Giroux et al. (1994) showed that these observations are incompatible with photoionization equilibrium by a single metagalactic ionizing background. In order to harmonize the theoretical predictions with the observations, they suggested that these LLSs poss a multi-phase interstellar medium similar to that of our Galaxy, in which extended hot, collisionally ionized gas is responsible for some or all of the high ionization stages of metal elements. On the other hand, Sciama (1994a, b) pointed out that decay neutrino photons together with soft X-ray bump from QSOs may produce the observed high $HeI/HI$ ratios and a wide distribution of column densities of C, N, and O ions.

## 5.7 Properties of the MASs

On the assumption that the MASs arise in galaxy halos, then the required cloud size can be determined if the number density of galaxies is known (as in Sargent et al. 1979). To do so, for instance, Lanzetta et al. (1987) adopted the galaxies luminosity function of Kirshner (1983) and further assumed that the halo radii scale with galaxy luminosity as $R \propto L^{0.4}$ and that all galaxies (not just spirals) participate in the absorption. For spherical halos, the required radius is then given by

$$R = 74(\frac{d\aleph}{dz})^{1/2}(1+z)^{-1/2}(1+2q_0z)^{1/4}\, h^{-1}kpc \qquad (5.10)$$

(Lanzetta et al. 1987; Bergeron 1988). The main results of average sizes of absorbers inferred in this way are listed in table 4.3. In the table 4.3. $R_H = 11h^{-1}kpc$ is the Holmberg (1975) radius averaged over the luminosity function.

Table 5.3. Estimates of Sizes

| | | system | $\bar{z}$ | $R/R_H$ |
|---|---|---|---|---|
| Lanzetta et al. | 1987 | MgII | 0.51 | 2.8 |
| | | MgII | 1.67 | 3.8 |
| Bergeron & Boissè | 1984 | CIV | 1.7 | 5.2 |
| Bechtold et al. | 1984 | LLS | 2 | 4.4 |

On the assumption of thermal equilibrium, the derived temperature of absorbers are the order of $\sim 10^4 K$. It is insensitive to the intensity of ionizing radiation within the reasonable range of $J_\nu$. However, a change of the spectral shape may introduce an uncertainty by a factor up to 3. Because the photoionization models are uniquely determined (except for the spectral shape far away from a power law) by the ionization parameter $U$, and because $U$ is essentially just the ratio of the incident intensity of radiation at the Lyman limit $J_{\nu_0}$ to the particle density $n_H$ in the cloud (see Eq.(5.4)), then $n_H$ can be determined if the values of $J_{\nu_0}$ and $U$ is known. As mentioned in the chapter 4, a estimate of $J_{\nu_0}$ at high redshifts has been made by BDO (1988). They suggest that $logJ_{\nu_0} = -21.0 \pm 0.5\, ergs^{-1}\, cm^{-2} Hz^{-1} Sr^{-1}$ over the redshift range $1.8 \leq z \leq 3.8$. However, several recent estimates of $J_{\nu_0}$ based on the proximity effect (Espey 1993; Bechtold 1994; Loeb & Eisentein 1995) showed that an uncertainty on $J_{\nu_0}$ of a factor of $\sim 3$ exists. For convenience of discussions, we define a variable $J_{21} = J_{\nu_0}/10^{-}21\, ergs^{-1}\, cm^{-2} Hz^{-1} Sr^{-1}$. On the basis of photoionization models, The particle density $n_H$ can then be expressed as a function of $U$ and $J_{21}$,

$$n_H = 6.3 \times 10^{-5} \frac{J_{21}}{U}\, cm^{-3}. \tag{5.11}$$

It can be seen immediately that, for $U \sim 10^{-3}$ and $J_{21} \sim 1$, the inferred gas density is $\sim 6.3 \times 10^{-2}\, cm^{-3}$. Once $n_H$ has been derived, the linear extent of the clouds, $R$, follows directly from the total hydrogen column density $N_H$, i.e. $R = N_H/n_H$. In terms of the quantities derived from the models,

$$R = 5.2 \frac{N_{20}(H) U_{-2}}{J_{21}} kpc. \tag{5.12}$$

where $N_{20}(H)$ is total hydrogen column density in unity of $10^{20}\,cm^{-2}$. However, the observed quantity is not total hydrogen, but neutral column density. Assumed photoionization equilibrium, $R$ may rewritten in terms of $N_{HI}$ below

$$R = 2.7\frac{N_{16}(HI)U_{-2}^2}{J_{21}}kpc. \tag{5.13}$$

If the clouds are assumed to be spherically symmetric radius $R/2$, the cloud mass is

$$M = 4.4 \times 10^7 N_{20}^2 U_{-2}^2 J_{21}^{-2} M_\odot. \tag{5.14}$$

Clearly, the sizes and masses are highly dependent on the parameters $N_H$ and $U$, which are derived from the photoionization models.

Taking $J_{21} \sim 1$ and adopting $U \sim 10^{-2}$ (Steidel 1990b), then the typical particle density in the clouds at redshift $z \sim 3$ is in the range $0.01 \leq n_H \leq 0.1\,cm^{-3}$, and the corresponding cloud sizes and masses are inferred to be in the range $1 \leq R \leq 15kpc$ and $10^6 \leq M_\odot \leq 10^9$, respectively.

On the other hand, at low redshif $z \sim 0.6-1$, the inferred particle density and size in CIV systems are $n_H \leq 3\times10^{-4}\,cm^{-3}$ and $R \geq 50kpc$, respectively. The MgII clouds have a density about 20 times higher than the CIV clouds and a size $R \sim 7kpc$.

## 5.8 Relationship between the MASs and Galaxies

Well before the absorber/galaxy connection was made directly, the MASs were widely believed to associate with galaxies because of a number of less-direct lines of evidence established from systematic studies of absorbers themselves (Bergeron 1988; Sargent et al. 1988, 1989). Firstly, the presence of elements heavier than He indicated that some star formation had occurred, even at very early epochs. Metal enriched by star formation generally implies the existence of a galaxies by definition. Secondly, when the MASs are observed at high spectral resolution, they almost always break up into sub-components with a typical velocity spread of $150 - 200\,kms^{-1}$. This was taken by some to imply their association with galaxy-sized objects. Lastly, the MASs are known to cluster on similar scales to galaxies ($\Delta v \leq 600\,kms^{-1}$; Sargent

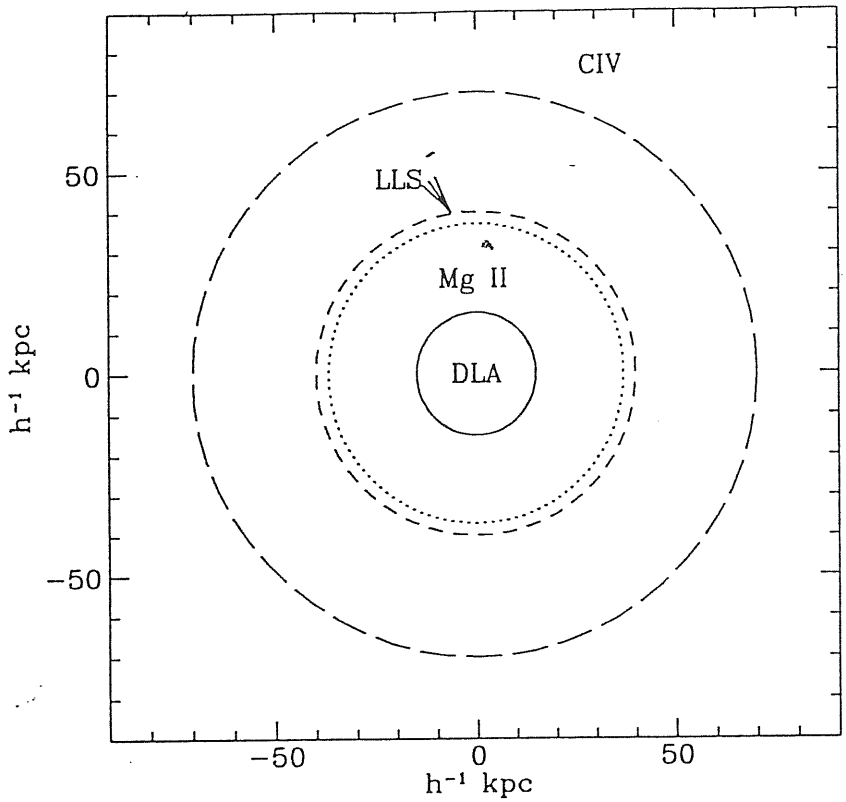


Figure 5.3: Schematic diagram illustrating an over-simplified view of the structure of a typical galaxy as deduced solely from the statistics of the various classes of metal-line absorption systems. Note that the MgII-selected and Lyman-limit systems have the same cross section, and that the damped Ly$\alpha$ systems have a cross section which is only a few percent of the total. Taken from Steidel (1993)

et al. 1988), and perhaps even on very large scales (e.g. Sargent et al. 1988; Heisler et al. 1989; Steidel & Sargent 1992).

Nevertheless, until the galaxies at high redshifts actually producing the absorption could be identified directly, it was not completely clear how the absorbers were related to the galaxies. Anyway, if assumed that the MASs associated with galaxies and normal galaxies were to account for enough cross section to produce the observed number of the MASs, it was clear early that each galaxy would have to have a gas cross section many times larger than the typical sizes of galaxies today. From the statistics of the incidence of the MASs alone, if one insists on producing the cross section using normal galaxies, a picture of a "typical" $L^*$ galaxy similar to the cartoon in Figure 5.3 is implied. The very large gaseous sizes implied by the statistics are responsible for the somewhat presumptuous term "halo gas" which often is used to refer to the sites giving rise to the bulk of the MASs.

By definition, the Damped Ly$\alpha$ systems refer to systems with $N(HI) \geq 3 \times 10^{20} cm^{-2}$, comparable to the typical column densities in the disks of spiral galaxies (see Wolfe et al. 1986; Lanzetta et al. 1991). The LLSs usually refer to systems which are just optically thick at the HI edge. An optical depth of unity or greater at the HI edge is also necessary to have appreciable column densities of MgII (see, e.g., Bergeron & Stasinska 1986); in fact, the LLSs and MgII-selected systems are essentially same population, and it is only because low-redshift MgII doublets can be detected using ground-based spectroscopy (whereas the LLSs require observations in the vacuum UV for redshfit $z < 2.5$) that many more MgII-selected systems are known for $z < 1$. The CIV-selected systems, which can have a very large range in $N(HI)$, have far the largest cross section, and have been found with $N(HI)$ as small as $10^{15.5} cm^{-2}$.

## 5.9 Comparison with the LCs

It is interesting to compare the properties of the MASs with those of the LCs. The inferred masses of the LCs are typically in the range $10^7 - 10^8 M_\odot$, remarkably similar to the range of masses of the MASs. The size of the LCs, set by observations of close QSO pairs and gravitationally lensed objects, is the order of $\sim 100 kpc$ (Bechtold et al. 1994; Smette et al. 1995; Dinshaw et al. 1995). This suggests that the LCs are in general larger and more dif-

fuse than the MASs. However, the coincidence in masses of the two types of absorbers suggests the possibility that they actually have similar origins (Tytler 1987), and the principle difference is just the gas density, and hence the ionization level.

Possibly the strongest demarkation between the LCs and the MASs is the difference in their clustering properties; as yet, no significant power in the velocity two-point correlation function has been found on scales $\geq 200\, kms^{-1}$ for the LCs, whereas there is significant clustering of the MASs on scales out to $\sim 600\, kms^{-1}$ (Sargent et al. 1988).

However, if one believes that the LCs really differ from the MASs only in density, one might argue that the extended, diffuse clouds could not exist in the vicinity of a galactic-size potential, because, for one, they would be tidally disrupted. Thus one might expect the small HI column density clouds would be to some extent *anticorrelated* with galaxies. A similar anticorrelation is expected if the clouds are gravitationally confined by "dark minihalos" (Rees 1986), or if the pressure of the ambient medium is too high in the vicinity of galaxies to allow the survival of the diffuse clouds if they are indeed pressure-confined. Indeed, on the scales less than $\leq 200\, kms^{-1}$, a positive correlation of the LCs with $logN_{HI} \geq 13.8$ has been confirmed (Cristiani et al. 1995a; Elowitz et al. 1995; Chernomordik 1995), but no correlation has been found yet for the small HI column density LCs.

On the other hand, a recent estimate of metallicity in the LCs by Cowie et al. (1995) is roughly $10^{-2}$ solar. This value is somewhat smaller than, but comparable to that of the MASs (a wide range of metallicity existing in the MASs). The metal abundance in the MASs would depend on galactocentric distance both because of changing particle densities (and thus HI columns) within the clouds and because of increased probabilities of cloud-cloud collisions which may induce star formation. Thus, the possibility exists that a continuum of metallicity exists, from the very diffuse LCs to the MASs with abundances comparable to the solar values.

In addition, the different redshift evolution of the low and high HI column density systems could be explained by proximity to galactic-sized potentials. The diffuse LCs may in fact be pressure confined by the ambient IGM, so that as the Universe expands they quickly evaporate, whereas the more dense clouds are presumably falling into the galactic potentials and becoming progressively more dense and more enriched in metal element. Thus, at lower redshfit, one might expect that most of the observed Lyman lines would

be associated with galaxies and therefore would begin to exhibit significant clustering on velocity scales of a few hundred $kms^{-1}$. Indeed, Mo & Morris (1994) and Lanzetta et al. (1994) found a significant association of the LCs with galaxies at low redshift. Moreover, low HI column density clouds would be expected to be extremely rare. However, unfortunately, the HST observations at very low redshfit reveal that the number density of the LCs is significantly larger than that extrapolated from the formula of the evolution of the LCs at high redshift (Bahcall et al. 1993a, b).

# Appendix: Curve of Growth Analysis

In order to derive an important property, column density, of the LCs from observational quantities, equivalent width and Doppler width, we must know the relationship among them. This field is traditionally called Curve of Growth Analysis.

Without considered the width of line, the line optical depth in terms of the atomic parameter is

$$\tau_0 = a_0 N, \tag{1}$$

where $a_0 = \frac{\pi e^2}{m_e c} f$ called an absorption coefficient for a line , $f$ is the oscillator strength. Actually, there are several mechanism to broaden line. For our case, both Doppler broadening and natural broadening (damping) are needed to take into account. In the case of natural broadening, arisen from the uncertainty principle, the absorption coefficient has the characteristic Lorentz shape

$$a(\lambda) = a_0 \frac{\gamma/4\pi^2}{(c/\lambda - c/\lambda_0)^2 + (\gamma/4\pi^2)^2}, \tag{2}$$

where $\gamma$ is the natural decay rate. On the other hand, in the case of Doppler broadening

$$a(\lambda) = \frac{a_0}{\pi^{1/2}} \frac{1}{\Delta\lambda_D} e^{-\Delta\lambda/\Delta\lambda_D{}^2}, \tag{3}$$

where $\Delta\lambda_D = \frac{b}{c}\lambda_0$, $b$ is the velocity. In above formula we have assumed an atom is in thermal equilibrium with an Gaussion distribution.

In the case of combination of Doppler broadening and damping, the net absorption coefficient as a function of frequency is given by the convolution of the two effects

$$a(\lambda_0) = a_0 \frac{-\lambda^2}{c\pi^{0.5}\Delta\lambda_D} H(\alpha, v). \tag{4}$$

where $H(\alpha, v) = \frac{\alpha}{\pi} \int_{-\infty}^{\infty} \frac{e^{-(v-u)^2}}{n^2-\alpha^2} du$ is known as the Voigt function. The definitions of $v$ and $\alpha$ given by $v = \frac{\Delta\lambda}{\Delta\lambda_D}$ and $\alpha = \frac{-\gamma\lambda_D{}^2}{4\pi c\Delta\lambda_D}$. At the center of line.

i.e. $v = 0$, we have $H(a, v) = 1$; so the opacity at the line center is

$$a(\lambda_0) = a_0 \frac{1}{\pi^{0.5} \Delta\lambda_D}. \tag{5}$$

The line opacity can be written

$$\frac{\tau(\lambda)}{\tau(\lambda_0)} = H(a, v). \tag{6}$$

Above equation describes the shape of absorption line. For comparison with measurement of absorption line, one usually introduces a variable, equivalent width, which indicates amount of absorption. To do this, first define the residual intensity given by

$$r(\lambda) = \frac{F_c - F(\lambda)}{F_c}, \tag{7}$$

where $F_c$ and F are the continuum flux and the measured flux respectively. The equivalent width W of the line in wavelength is then given by

$$W = \int_0^\infty r(\lambda) d\lambda. \tag{8}$$

In the case of the IGM, the curve of growth may be divided into three distinct region:

1. Linear Region

   It locates in the region with column density $N \leq 10^{15}\, cm^{-2}$. The equivalent widths are proportional to column density.

2. Saturated Zone

   It locates in the region of $10^{15} < N < 10^{18}\, cm^{-2}$. $W$ grows extremely slow with increasing of column density ($W \propto logN$), so called saturated zone.

3. Damping Wing

   As $N > 10^{18}\, cm^{-2}$, damping dominates the line broadening, the equivalent width W grows again as $N^{1/2}$.

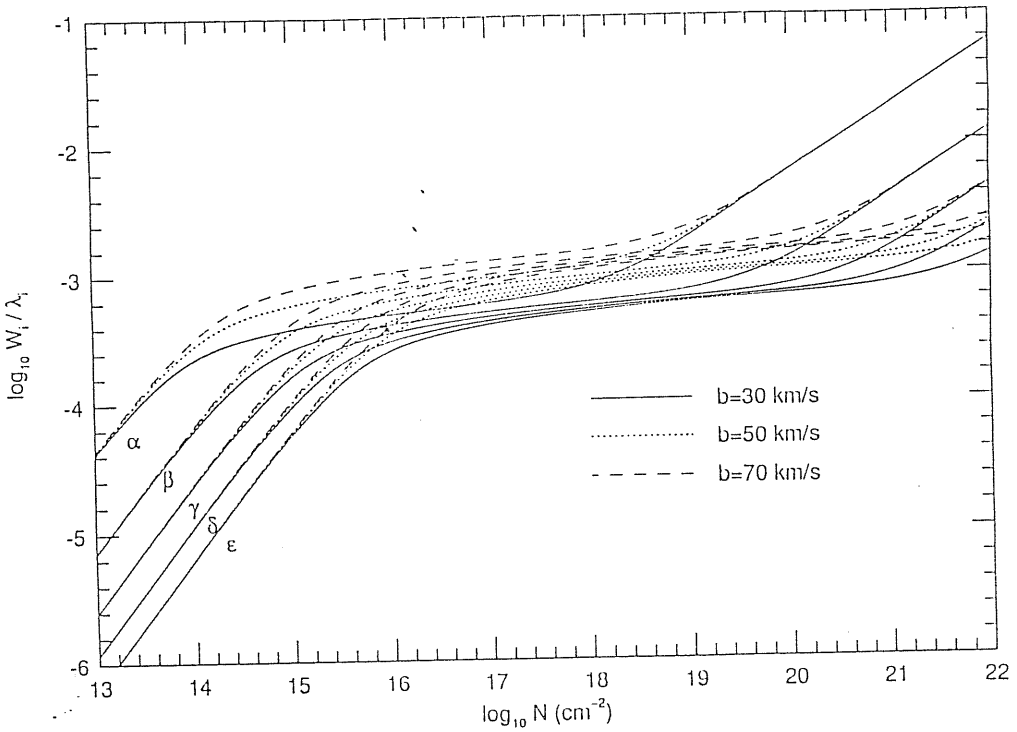


Figure 1: Equivalent width $W$ for Lyman series lines in hydrogen as as a function of column density $N$ and thermal velocity parameter $b$. Equivalent widths grow linearly with N in the unsaturated region below $N \sim 10^{14-15}\, cm^{-2}$, until they saturate at a value set the thermal Doppler width. In the saturated zone, widths grow slowly as $\sim log^{1/2}N$. In the damping wing, of HI (curve of growth) including saturation, widths grow as $\sim N^{1/2}$. Taken from Press et al. (1993).

# References


[1] Aldcroft, T.L., Bechtold, J., & Elvis, M., 1994, ApJS, 93, 1

[2] Atwood, B., Baldwin, J.A., & Carswell, R.F. 1985, ApJ, 292, 58

[3] Babul, A., Rees, M.J., 1992, MNRAS, 255, 346

[4] Bahcall, J.N., & Peebles, P.J.E., 1969, ApJ, 156, L7

[5] Bahcall, J.N., et al. 1991, ApJ, 377, L5

[6] Bahcall, J.N., et al. 1992a, ApJ, 397, 68

[7] Bahcall, J.N., et al. 1992b, ApJ, 398, 495

[8] Bahcall, J.N., et al. 1993a, ApJS, 87, 1

[9] Bahcall, J.N., Jannuzi, B.T., Schneider, D.P., & Hartig, G.F., 1993b. ApJ, 405, 491

[10] Bajtlik, S., Duncan, R.C., & Ostriker, J.P. 1988, ApJ, 327, 570 (BDO)

[11] Barcons, x., & Fabian, A.C., 1987, MNRAS, 224, 674

[12] Barcons, x., Fabian, A.C., & Rees, M.J. 1991, Nature, 350, 685.

[13] Barcons, x., & Webb, J.K. 1991, MNRAS, 253, 207

[14] Baron, E., Carswell, R.F., Hogan, C.J., & Weymann, R.J., 1989. ApJ, 337, 609

[15] Beaver, E.A., et al. 1991, ApJ, 337, L1

[16] Bechtold, J., et al. 1984, ApJ, 281, 76

[17] Bechtold, J., Weymann, R.L., Liu, Z., & Malkan, M. 1987, ApJ, 315, 180

[18] Bechtold, J., 1988, Mount Wilson and Los Campanas, preprint

[19] Bechtold, J., 1994, ApJS, 91, 1

[20] Bechtold, J., Crotts, A.P.S., Duncan, R.C., & Fang, Y., 1994, 437, L83

[21] Bergeron, J., & Boissè, P. 1984, A&A, 133, 374

[22] Bergeron, J., & Stasinska, G., 1986, A&A, 169, 1

[23] Bergeron, J., 1988, QSO absorption lines: Probing the Universe, ed. C.Blades, D.Turnshek, C,Norman (Cambridge: Cambridge Univ. Press), p. 127

[24] Bergeron, J., & Boissè, P. 1991, A&A, 243, 344

[25] Bergeron, J., et al. 1994, ApJ, 436, 33

[26] Black, J.H., 1981, MNRAS, 197, 553

[27] Black, J.H., Chaffee, F.H.Jr., & Foltz, C.B., 1987, ApJ, 317, 442

[28] Blades, J.C., Hunstead, R.W., Murdoch, H.S., & Pettini, M., 1982, MNRAS, 200, 291

[29] Blades, J.C., 1988, QSO absorption lines: Probing the Universe, ed. C.Blades, D.Turnshek, C,Norman (Cambridge: Cambridge Univ. Press), p. 147

[30] Boksenberg, A., 1995, in ESO Workshop, QSO Absorption lines, ed. G. Meylan (Garching: European Southern Observatory), in press

[31] Bond, J.R., Szalay, A.S., & Silk, J., 1988, ApJ, 324, 627

[32] Boyle, B.J., Jones, L.R., & Shanks, T. 1991, MNRAS, 251, 482

[33] Carswell, R.F., Weelan, J.A.J., Smith, M.G., Boksenberg, A., & Tytler, D. 1982, MNRAS, 198, 91

[34] Carswell, R.F., et al. 1984, ApJ, 278, 486

[35] Carswell, R.F., Webb, J.K., Baldwin, J.A., & Atwood, B. 1987, ApJ, 319, 709

[36] Carswell, R.F., Lanzetta, K.M., Parnell, H.C., & Webb, J.K. 1991, ApJ, 371, 36

[37] Carswell, R.F., Mauch, M., Weymann, R.J., Cooke, A.J., Webb, J.K., 1994, MNRAS, L1

[38] Cen, R.Y., Jameson, A., Liu, F., & Ostriker, J.P., 1990, ApJ, 362, L41

[39] Cen, R.Y., Ostriker, J.P., 1993, ApJ, 417, 404

[40] Cen, R.Y., Miralda-Escudé, J., Ostriker, J.P., & Rauch, M., 1994, ApJ, 437, L9

[41] Chaffee, F.H.Jr., Weymann, R.J., Latham, D.W., & Strittmatter, P.A., 1983, ApJ, 267, 12

[42] Chaffee, F.H.Jr., Foltz, C.B., Röser, H.J., Weymann, R.J., & Latham, D.W., 1985, ApJ, 292, 362

[43] Chaffee, F.H.Jr., Foltz, C.B., Bechtold, J., & Weymann, R.J., 1986, ApJ, 301, 116

[44] Charlton, J.C., Salpeter, E.E., & Hogan, C.J., 1993, ApJ, 402, 493

[45] Charlton, J.C., Salpeter, E.E., & Linder, S.M., 1994, 430, L29

[46] Chernomordik, V.V., & Ozernoy, L.M., 1983, Nature, 303, 153

[47] Chernomordik, V.V., 1995, ApJ, 440, 431

[48] Chiang, W.H., Ryu, D., & Vishniac, E.T. 1989, ApJ, 339, 603

[49] Code, A.D., & Welch, G.A. 1982, ApJ, 256, 1

[50] Cowie, L.L., Songaila, A., Kim, T.S., & Hu, E.M., 1995, Astron.J., 109, 1522

[51] Cristiani, S., Giallongo, E., Buson, L.M., Gouiffes, C., & Franca, F.L., 1993, A&A, 268, 86

[52] Cristiani, S., D'Odorico, S., Fontana, A., Giallongo, E., & Savaglio, S., 1995a, MNRAS, 273, 1016

[53] Cristiani, S., et al. 1995b, preprint

[54] Crotts, A.P.S., 1987, MNRAS, 228, 41p

[55] Crotts, A.P.S., 1989, ApJ, 336, 550

[56] Dinshaw, N., Impey, C.D., Fotlz, C.B., Weymann, R.J., & Chaffee, F.H.Jr., 1994, ApJ, 437, L87

[57] Dinshaw, N., Fotlz, C.B., Impey, C.D., Weymann, R.J., & Morris, S.L., 1995, in ESO Workshop, QSO Absorption lines, ed. G. Meylan (Garching: European Southern Observatory), in press

[58] Dobrzycki, A., & Bechtold, J., 1991, ApJ, 377, L69

[59] D'Odorico, S., Molaro, P., & Savaglio, S., 1991, in Proceedings of the ESO Mini Workshop on Quasar Absorption Lines, ed. P.A. Shaver, E.J. Wampler & A.M. Wolfe (ESO Scientific Report No. 9 - February 1991), 15

[60] Donahue, M.J., & Shull, J.M. 1987, ApJ, 323, L13

[61] Dragovan, M., et al. 1994, ApJ, 427, L67

[62] Duncan, R.C., Ostriker, J.P., & Bajtlik, S., 1988, ApJ, 345, 39

[63] Duncan, R.C., Vishniac, E.T., & Ostriker, J.P., 1991, ApJ, 368, L1

[64] Ellis, R.S. 1978, MNRAS, 185, 613

[65] Elowitz, R.M., Green, R.F., & Impey, C.D., 1995, ApJ, 440, 458

[66] Espey, B.R., 1993, ApJ, 411, L59

[67] Fall, S.M., & Pei, Y.C. 1993, ApJ, 402, 479

[68] Fang, Y., & Crotts, A. 1995, ApJ,

[69] Field, G.B. 1959, ApJ, 129, 536

[70] Field, G.B. 1972, ARA&A, 10, 227

[71] Foltz, C.B., Weymann, , R.J., Roser, H.J., & Chaffee. F.H.Jr., 1984, ApJ, 281, L1

[72] Foltz, C.B., et al. 1986, ApJ, 307, 504

[73] Foltz, C.B., Chaffee. F.H.Jr., & Black. J.H., 1988, ApJ, 324, 267

[74] Giallongo, G. & Cristiani, S., 1990, MNRAS, 247, 696

[75] Giallongo, G., Cristiani, S., & Trevese, D., 1992, ApJ, 398, L9

[76] Giallongo, G., Cristiani, S., Fantana, A., & Trevese, D., 1993, ApJ. 412, 64

[77] Giallongo, G., et al. 1994, ApJ, 425, L1

[78] Giroux, M.L., & Shapiro, P.R., 1994, preprint

[79] Giroux, M.L., Fardal, M.A., & Shull, M. 1995, preprint

[80] Guun, J.E., & Peterson, B.A. 1965, ApJ, 142, 1633

[81] Heisler,J., Hogan, C., & White, S.D.M., 1989, ApJ, 347, 52

[82] Hewett, P.C., Foltz, C.B., & Chaffee, F.H. 1993, ApJ, 406, L43

[83] Hoffman, G.L., Lu, N.Y., & Salpeter, E.E., et al. 1993, AJ, 106, 39

[84] Holmberg, E., 1975, in Galaxies and the Universe, ed. A.Sandage, M.Sandage, & J.Kristian (University Press:Chicago), P. 123

[85] Hunstead, R.W., Prttini, M., Blades, J.C., & Murdoch, H.S. 1987a, Proceedings of IAU Symposium 124, Observational Cosmology, ed. A. Hewitt, G. Burbidge, & L.Z. Fang, p. 799

[86] Hunstead, R.W., Murdoch, H.S., Prttini, M., & Blades, J.C., 1987b, ApJ, submitted

[87] Hunstead, R.W., 1988, QSO absorption lines: Probing the Universe, ed. C.Blades, D.Turnshek, C.Norman (Cambridge: Cambridge Univ. Press), p. 71

[88] Hunstead, R.W., 991, in Proceedings of the ESO Mini Workshop on Quasar Absorption Lines, ed. P.A. Shaver, E.J. Wampler & A.M. Wolfe (ESO Scientific Report No. 9 - February 1991), 11

[89] Ikeuchi, S., Tomisaka, K., & Ostriker, J.P., 1983, ApJ, 265, 583

[90] Ikeuchi, S., 1986, As&SS, 118, 509

[91] Ikeuchi, S., & Ostriker, J.P. 1986, 301, 522

[92] Ikeuchi, S., Murikama, I., & Rees, M.J., 1988 MNRAS, 236, 21p

[93] Irwin, M., McMahon, R.G., & Hazard, C. 1991,

[94] Jakobsen, P. 1980, A&A, 81, 66

[95] Jakobsen, P., et al. 1993, ApJ, 417, 528

[96] Jakobsen, P., et al. 1994, Nature, 370, 35

[97] Jenkins, E.B., 1991, in Proceedings of the ESO Mini Workshop on Quasar Absorption Lines, ed. P.A. Shaver, E.J. Wampler & A.M. Wolfe (ESO Scientific Report No. 9 - February 1991), 25

[98] Jenkins, E.B., & Ostriker, J.P., 1991, ApJ, 376, 33

[99] Kulkarni, V.P., & Fall, S.M., 1993, ApJ, 413, L63

[100] Kulkarni, V.P., Huang, K.L., Green, R.F., et al. 1994, ApJ, submitted

[101] Kurt, V.G., & Sunyaev, R.A. 1967, Cosmic Research, 5, 496

[102] Lanzetta, K.M., Turnshek, D.A., & Wolfe, A.M. 1987, ApJ, 322, 739

[103] Lanzetta, K.M. 1988, ApJ, 332, 96

[104] Lanzetta, K.M., Wolf, A.M., & Turnshek, D.A., 1989 ApJ, 344, 277

[105] Lanzetta, K.M. 1991, ApJ, 375, 1

[106] Lanzetta, K.M., Wolfe, A.M., Turnshek, D.A., Lu, L., McMahon, R.G., & Hazard, C. 1991, ApJS, 77, 1

[107] Lanzetta, K.M., Turnshek, D.A., &Sandoval, J., 1992, ApJS, 75, 645

[108] Lanzetta, K.M., Bower, D.V., Tytler, D., Webb, J.K., & Sealey, K.M., 1995, ApJ, in press

[109] Loeb, A., & Eisenstein, D., 1995, preprint

[110] Lu, L., Wolfe, A.M., & Turnshek, D.A., 1991, 367, 19

[111] Lu, L., 1991, ApJ, 379, 99

[112] Lu, L., Wolfe, A.M., Turnshek, D.A., & Lanzetta, K.M., 1993, ApJS, 84, 1

[113] Lynds, C.R. 1971, ApJ, 164, L73

[114] Madau, P. 1991, ApJ, 376, L33

[115] Madau, P. 1992, ApJ, 389, L1

[116] Madau, P., & Meiksin, A. 1991, ApJ, 374, 6

[117] Madau, P., & Meiksin, A. 1994, ApJ, 433, L53

[118] Mather, J.C., et al. 1994, 420, 439

[119] Meiksin, A., & Madau, P. 1993, ApJ, 412, 34

[120] Meiksin, A., 1994, ApJ, 431, 109

[121] Meyer, D.M., & York, D.G., 1987, ApJ, 315, L5

[122] Miralda-Escudé, J., & Ostriker, J.P. 1990, ApJ, 350, 1

[123] Miralda-Escudé, J., & Ostriker, J.P. 1992, ApJ, 392, 15

[124] Miralda-Escudé, J., & Rees, M.J., 1993, MNRAS, 260, 617

[125] Miralda-Escudé, J. 1993, MNRAS, 262, 273

[126] Miralda-Escudé, J. 1994, MNRAS, 266, 343

[127] Mo, H.J., Miralda Miralda-Escudé, J., & Rees, M.J., 1993, MNRAS, 264, 705

[128] Mo, H.J., & Morris, S.L., 1994, MNRAS, 269, 52

[129] Møller, P., & Jakobsen, P. 1990, A&A, 228, 299

[130] Møller, P., & Kjærgaard, P., 1992, A&A, 258, 234

[131] Møller, P., Jakobsen, P., & Perryman, M.A.C., 1994, A&A, 287, 719

[132] Morris, S.L., Weymann, R.J., Savage, B.D., & Gilliland, R.L., 1991, ApJ, 377, L21

[133] Morris, S.L., et al. 1993, ApJ, 419, 524

[134] Morris, S.L., & Bergh, S.V.D., 1994, ApJ, 427, 696

[135] Murdoch, H.S., Hunstead, R.W., Pettini, M., & Blades, J.C. 1986, ApJ, 309, 19 (MHPB)

[136] Murikama, I., & Ikeuchi, S., 1993, 409, 42

[137] Nath, B.B., & Biermann, D.L. 1993 MNRAS, 265, 241

[138] Norris, J., Hartwick, F.D.A., & Peterson, B.A., 1983 ApJ, 273, 450

[139] Ostriker, J.P., & Ikeuchi, S. 1983, ApJ, 268, L63

[140] Ostriker, J.P., & Heisler, J. 1984, ApJ, 278, 1

[141] Ostriker, J.P., Bajtlik, S., & Duncan, R.C., 1988, ApJ, 327, L35

[142] Ostriker, J.P. 1988, QSO absorption lines: Probing the Universe, ed. C.Blades, D.Turnshek, C,Norman (Cambridge: Cambridge Univ. Press), p. 319

[143] Paresce, F., McKee, C., & Bowyer, S. 1980, ApJ, 240, 387

[144] Peterson, B.A. 1978, proceedings of IAU Symposium 79, The Large Scale Structure of the Universe, ed. M.S. Longair & J. Einasto, P. 309

[145] Peterson, B.A. 1983a, proceedings of IAU Symposium 104, Early Evolution of the Universe and its Present Structure, eds. G.O. Abell & G. Chincarini, P. 349

[146] Peterson, B.A. 1983b, in Proc. 24th Liége Internat. Colloquium. Qsosars and Gravitational Lenses, ed. J.P. Swings, p. 349

[147] Petitjean, P., & Bergeron, J., 1990, A&A, 265, 375

[148] Petitjean, P., Boisson, C., & Péquignot, D., 1990, A&A, 240, 433

[149] Petitjean, P., Bergeron, J., & Puget, J.L., 1992, A&A 265, 375

[150] Petitjean, P., Bergeron, J., Carswell, R.F., & Puget, J.L., 1993b, MNRAS, 260, 67

[151] Petitjean, P., Webb, J.K., Rauch, M., Carswell, R.F., Lanzetta, K., 1993a, MNRAS, 262, 499

[152] Petitjean, P., Rauch, M., & Carswell, R.F., 1994, A&A 291, 29

[153] Pettini, M., Hunstead, R.W., murdoch, H.S., & Blades, J.C., 1983, ApJ, 273, 463

[154] Pettini, M., Hunstead, R.W., Smith, L.J., & Mar, D.P., 1990a, MNRAS, 246, 545 (PHSM)

[155] Pettini, M., Boksenberg, A., & Hunstead, R.W., 1990b, ApJ, 348, 48

[156] Pettini, M., Smith, L.J., Hunstead, R.W., & King, D.L., 1994, ApJ, 426, 79

[157] Phillips, S., & Ellis, R.S. 1983, MNRAS, 204, 493

[158] Press, W.H., Rybicki, G.B., & Schneider, D.P., 1993, ApJ, 414, 64

[159] Rauch, M., Carswell, R.f., Chaffee, F.H., Foltz, C.B., Webb, J.K., Weymann, R.J., Bechtold, J., & Green, R.F. 1992, ApJ, 390, 387

[160] Rauch, M., Carswell, R.f., Webb, J.K., 1993, & Weymann, R.J., 1993 MNRAS, 260, 589

[161] Readhead, A.C.S., et al. 1989, ApJ, 346, 566

[162] Rees, M.J., & Setti, G. 1970, A&A, 8, 410

[163] Rees, M.J. 1986, MNRAS, 218, 25P

[164] Rees, M.J. 1988, QSO absorption lines: Probing the Universe, ed. C.Blades, D.Turnshek, C,Norman (Cambridge: Cambridge Univ. Press), p. 107

[165] Reimers, D., et al. 1992, Nature, 360, 561

[166] Reimers, D., & Vogel, S. 1993, A&A, 276, L13

[167] Ryu, D., Vishniac, E.T., & Chiang, W.H. 1990, ApJ, 309

[168] Salpeter, E.E., 1993, AJ, 106, 1265

[169] Salpeter, E.E., 1994, preprint

[170] Salpeter, E.E., Hoffman, G.J., 1995, ApJ, 441, 51

[171] Sargent, W.L.W., Young, P.J., Boksenberg, A., & Tytler, D. 1980, ApJS, 42, 41 (SYBT)

[172] Sargent, W.L.W., & Boksenberg, A. 1983b, in Proc. 24th Liége Internat. Colloquium, Qsosars and Gravitational Lenses, ed. J.P. Swings, p. 518

[173] Sargent, W.L.W., Boksenberg, A., & Steidel, C.C. 1988, ApJS, 68, 539

[174] Sargent, W.L.W., Steidel, C.C. & Boksenberg, A., 1988, ApJ, 334, 22

[175] Sargent, W.L.W., Steidel, C.C. & Boksenberg, A., 1989, ApJS., 69, 639-703-761

[176] Savaglio, S., & Webb, J., 1995, preprint

[177] Schmidt, M., Schneider, D.P., & Gunn, J.E. 1991, in ASP conf. Ser. 21, The Space Distribution of Quasars, ed. D. Crampton (San Francisco: ASP), 109

[178] Schneider, D.P., Schmidt, M., & Gunn, J.E. 1989, A.J., 98, 1507

[179] Sciama, D.W. 1990, ApJ, 364, 549

[180] Sciama, D.W. 1990, Phys.Rev.Lett., 65, 2839

[181] Sciama, D.W. 1990, Nature, 346, 40

[182] Sciama, D.W. 1993, Modern Cosmology and the Dark Matter Problem, Cambridge University Press

[183] Sciama, D.W. 1994a, ApJ, 422, L49

[184] Sciama, D.W. 1994b, ApJ, 426, L65

[185] Shapiro, P.R. 1986, PASP, 98, 1014

[186] Shapiro, P.R., & Giroux, M.L. 1987, ApJ, 321, L107

[187] Shapiro, P.R., Giroux, M.L., & Babul, A. 1991, in After the First Three Minutes, ed. S.S.Holt,C.L.Bennett, & V.Trimble (New York:AIP), 347

[188] Shapiro, P.R., & Giroux, M.L., & Babul, A., 1994, ApJ, 427, 25

[189] Shaver, P.A., & Robertson, J.G., 1983, ApJ, 268, L57

[190] Sherman, R.D. 1980a, ApJ, 237, 355

[191] Sherman, R.D. 1980b, ApJ, 238, 749

[192] Sherman, R.D. 1980c, ApJ, 240, 737

[193] Sherman, R.D. 1982, ApJ, 256, 370

[194] Smette, A., Surdej, J., Shaver, P.A., et al. 1992, ApJ, 389, 39

[195] Smette, A., 1995, in ESO Workshop, QSO Absorption lines, ed. G. Meylan (Garching: European Southern Observatory), in press

[196] Smoot, G.F., et al. 1992, ApJ, 396, L1

[197] Songaila, A., Cowie, L.L., & Lilly, S.J. 1990 ApJ, 348, 371

[198] Songaila, A., Cowie, L.L., Hogan, C.J., & Rugers, M., 1994, Nature, 368, 599

[199] Stebbins, A., & Silk, J. 1986, ApJ, 300, 1

[200] Steidel, C.C., & Sargent, W.L.W. 1987a, ApJ, 313, 171

[201] Steidel, C.C., & Sargent, W.L.W. 1987b, ApJ, 318, L11

[202] Steidel, C.C., & Sargent, W.L.W. 1989, ApJ, 343, L33

[203] Steidel, C.C. 1990a, ApJS, 72, 1

[204] Steidel, C.C. 1990b, ApJS, 74, 37

[205] Steidel, C.C., & Sargent, W.L.W., 1992, ApJS, 80, 1

[206] Steidel, C.C., 1993, the Environment and Evolution of Galaxies (Kluwer, Dordrecht), eds, J.M.Shull & H.A.Thronson, p. 263

[207] Storrie-Lombardi, J.L., McMahon, R.G., Irwin, M.J., & Hazard, C., 1994, ApJ, 427

[208] Strömgren, B. 1939, ApJ, 89, 529

[209] Terasawa, N. 1992, ApJ, 392, L15

[210] Tripp, T.M., Green, R.F., & Bechtold, J. 1990, ApJ, 364, L29

[211] Tytler, D. 1982, Nature, 298, 427

[212] Tytler, D. 1987, ApJ, 321, 49

[213] Tytler, D., Boksenberg, A., Sargent, W.L.W., Young, P., & Kunth, D. 1987, ApJS, 64, 667

[214] Tytler, D., & Fan, X., 1994, ApJ, 424, L87

[215] Tytler, D., 1995, in ESO Workshop, QSO Absorption lines, ed. G. Meylan (Garching: European Southern Observatory), in press

[216] Vogel,S., & Reimer, D., 1995, A&A, 294, 410

[217] Walker, T.P., Steigman, G., Schramm, D.N., Olive, K.A., & Kang, H.S. 1991, ApJ, 376, 51

[218] Wang, B., 1995, ApJ Letters, in press

[219] Warren, S.J., Hewett, P.C., & Osmer, P.S. 1991, in ASP conf. Ser. 21, The Space Distribution of Quasars, ed. D. Crampton (San Francisco: ASP), 139

[220] Webb, J.K., 1987a, proceedings of IAU Symposium 124, Observational Cosmology, ed. A. Hewitt, G. Burbidge, & L.Z. Fang, p, 799

[221] Webb, J.K., & Carswell, R.F., 1991, in Proceedings of the ESO Mini Workshop on Quasar Absorption Lines, ed. P.A. Shaver, E.J. Wampler & A.M. Wolfe (ESO Scientific Report No. 9 - February 1991), 3

[222] Webb, J.K., & Barcons, X., 1991, MNRAS, 186, 145

[223] Webb, J.K., Barcons, X., Carswell, R.F., & Paenell, H.C. 1992, MNRAS, 255, 319

[224] Weymann, R.J. 1967, ApJ., 887

[225] Weymann, R.J., Williams, R.E., Peterson, B.M., & Turnshek, D.A., 1979, ApJ, 226, 603

[226] Weymann, R.J., carswell, R.F., & Smith, M.G. 1981, ARAA 19, 41

[227] Weymann, R.J., & Foltz, C.B. 1983, ApJ, 272, L1

[228] Williger, G.M., & Babul, A., 1992, 399, 385

[229] Wolfe, A.M., Turnshek, D.A., Smith, H.E., & Cohen, R.D. 1986, ApJS., 61, 249

[230] Wolfe, A.M., Lanzetta, K.M., & Oren, A.L., 1992, ApJ, 388, 17

[231] Wolfe, A.M., Turnshek, D.A., Lanzetta, K.M., & Lu, L., 1993, ApJ, 404, 480

[232] York, D.G., Green, R.F., Bechtold, J., & Chaffee, F.H.Jr., 1984, ApJ, 280, L1

[233] Young, P., Sargent, W.L.W., & Boksenberg, A. 1982, ApJ, 252, 10

[234] Young, P., Sargent, W.L.W., & Boksenberg, A. 1982, ApJS, 48, 455

[235] Zheng, W., & Davidsen, A. 1995, ApJ, 440, L53

[236] Zou, Z.L., et al. 1982, Acta.Astrophys.Sin., 2, 252 [translated in Chin.Astr.Ap., 7, 31 (1983)]